



**Queensland University of Technology**  
Brisbane Australia

This may be the author's version of a work that was submitted/accepted for publication in the following source:

[Steau, Edward & Mahendran, Mahen](#)  
(2021)

Elevated temperature thermal properties of fire protective boards and insulation materials for light steel frame systems.

*Journal of Building Engineering*, 43, Article number: 102571.

This file was downloaded from: <https://eprints.qut.edu.au/209748/>

© 2021 Elsevier Ltd.

This work is covered by copyright. Unless the document is being made available under a Creative Commons Licence, you must assume that re-use is limited to personal use and that permission from the copyright owner must be obtained for all other uses. If the document is available under a Creative Commons License (or other specified license) then refer to the Licence for details of permitted re-use. It is a condition of access that users recognise and abide by the legal requirements associated with these rights. If you believe that this work infringes copyright please provide details by email to [qut.copyright@qut.edu.au](mailto:qut.copyright@qut.edu.au)

**License:** Creative Commons: Attribution-Noncommercial-No Derivative Works 4.0

**Notice:** *Please note that this document may not be the Version of Record (i.e. published version) of the work. Author manuscript versions (as Submitted for peer review or as Accepted for publication after peer review) can be identified by an absence of publisher branding and/or typeset appearance. If there is any doubt, please refer to the published source.*

<https://doi.org/10.1016/j.jobbe.2021.102571>

# **Elevated Temperature Thermal Properties of Fire Protective Boards and Insulation Materials for Light Steel Frame Systems**

Edward Steau and Mahen Mahendran  
*Queensland University of Technology (QUT), Brisbane, Australia*

**Abstract:** New materials are increasingly used in the construction of cold-formed Light gauge Steel Frame (LSF) systems to achieve lightweight, more durable and fire resistant building systems. However, these materials are being used without good knowledge and understanding of their elevated temperature thermal properties. Hence a thorough investigation of the elevated temperature thermal properties was conducted for a range of building materials used in the LSF systems of Australia, New Zealand and Europe. Thermal property tests were conducted on gypsum plasterboards, calcium silicate boards, magnesium oxide boards, perlite boards, insulation materials and structural plywoods, totalling 21 potential LSF components. The thermal properties of specific heat at constant pressure, relative density, thermal conductivity and thermal diffusivity were determined using differential scanning calorimetry, thermogravimetric analysis and laser flash analysis and the guidelines of ASTM standard test methods. This paper presents the results of the elevated temperature thermal properties of a range of building materials used in the LSF systems. This advanced knowledge and understanding of the elevated temperature thermal properties will allow accurate predictions of the fire resistance of LSF systems using appropriate numerical and fire design methods and facilitate the development of improved LSF systems with enhanced fire resistance levels. Several materials such as gypsum plasterboards, calcium silicate boards, perlite board and rockwool fibre insulation have been identified to be suitable for use in LSF systems because of their high specific heat, low thermal conductivity, reduced mass loss and low bulk density.

**Keywords:** *LSF systems; Thermal properties; Specific heat; Relative density; Thermal conductivity.*

## **1. Introduction**

Fire safety design of Light gauge Steel Frame (LSF) wall and floor systems relies on good knowledge and understanding of the elevated temperature thermal characteristics of their component materials. In order to predict the fire behaviour accurately and to improve the thermal performance of LSF systems, accurate elevated temperature thermal properties of all their component materials are required. These thermal properties include specific heat at

constant pressure ( $C_p$ ), relative density ( $\rho$ ), thermal conductivity ( $\lambda$ ) and thermal diffusivity ( $\alpha$ ) [1-3].

LSF systems are protected against fire action through the use of fire resistant boards. The most commonly used fire resistant board in LSF systems is gypsum plasterboard due to its non-combustible core and fire-resisting properties. The gypsum plasterboard core is predominantly gypsum (calcium sulphate dihydrate ( $\text{CaSO}_4 \cdot 2\text{H}_2\text{O}$ )), a naturally occurring non-combustible mineral, and is sandwiched between two sheets of heavy duty recycled paper. These boards contain about 20.9% chemically bound water with 3-4% free moisture content. Significant heat energy is needed to evaporate the free water and to make the chemical change that releases the water in the crystal structure. When exposed to fire, many reactions occur in gypsum plasterboards, delaying the heat transfer to the wall/floor frames [4,5].

Significant amount of research has been undertaken on gypsum plasterboards in relation to their elevated temperature thermal properties, material characteristics, phase transitions due to chemical decomposition reactions, chemical/ingredient compositions and manufacturing procedures [6-8]. However, in recent times alternative fire rated boards, are being used with LSF systems with claims that they are superior to gypsum plasterboards. However, for many of these alternative fire rated boards, their thermal properties are either not available as a function of temperature or many uncertainties exist in regard to the data provided. Therefore in this research a detailed experimental study was undertaken on a range of fire resistant boards, insulation materials and other boards such as plywood used in LSF systems. Following list gives their details:

- **Calcium Silicate Boards:** Calcium silicate is the main material used in these boards. Depending on hydrothermal synthesis conditions, different calcium silicate phases can be synthesised. These products can differ based on crystalline structure and chemically bonded water ((OH)<sub>2</sub> groups and or H<sub>2</sub>O molecules) and include Tobermorite ( $\text{Ca}_5\text{Si}_6\text{O}_{16}(\text{OH})_2 \cdot 4\text{H}_2\text{O}$ ), Xonotlite ( $\text{Ca}_6\text{Si}_6\text{O}_{17}(\text{OH})_2$ ) and Wollastonite ( $\text{CaSiO}_3$ ). The calcium silicate hydrates are obtained by a hydrothermal synthesis of an aqueous suspension of lime and silica [9,10]. Their density classifies commercial calcium silicate boards into three categories, i.e. boards of low density (200 to 500 kg/m<sup>3</sup>), medium density (500 to 1000 kg/m<sup>3</sup>) and high density (1000 to 1800 kg/m<sup>3</sup>) [10].

- Magnesium Oxide Boards: These rigid boards are made with additional reinforcing fibreglass mesh on the outer face instead of paper layers. The main core material is Magnesium Oxide (MgO), a naturally occurring material in the form of magnesite (magnesium carbonate – MgCO<sub>3</sub>) and magnesium chloride (MgCl<sub>2</sub>), obtained from rich brine and sea water [11].
- Perlite Boards: Perlite is the main material, which is an amorphous volcanic glass that when sufficiently heated expands to form enclosed hollow spheres. Perlite boards are lightweight, easy to handle, and provide low cost, high strength and chemical stability. Perlite is also used in other products due to their low density, for example, lightweight plasterboard, concrete, masonry and insulation boards.
- Insulation Materials: Glass fibre, Rockwool fibre, Cellulose fibre and three types of Aerogel insulation materials are used in this study. Aerogel insulation materials are used as high performance insulations due to their low thermal conductivity. Silica aerogels are synthesised by a three-step process, which includes gel preparation by sol–gel processes, ageing of gel in solution to prevent it from shrinking during drying, and drying of gel under supercritical drying to prevent the collapse of gel structure [12].
- Structural Plywood: In this engineered structural product, timber veneers are permanently cross-laminated together using the permanent Type A bond [13]. It is composed of a mixture of cellulose, hemicellulose and lignin bound together in a complex network [14]. In this study two different structural plywoods of F8 and F11 Stress Grades were considered due to their use as subfloor linings in LSF floor-ceiling systems. However, at elevated temperatures rapid pyrolysis occurs in wood and combustion will follow making the subfloor lining of structural plywoods vulnerable in a fire rated LSF floor-ceiling systems.

This paper presents the details of an experimental study on the elevated temperature thermal properties of the above-mentioned building materials used in Australia, New Zealand and Europe, and the results. Twenty one boards and insulation materials of varying types and compositions were sourced from different manufacturers and tested using thermal analysis instruments (Tables 1 and 2) and ASTM E1269 [15] and ASTM E1461 [16] standard test methods. These tests were conducted using differential scanning calorimetry, thermogravimetric analysis and laser flash analysis to obtain the results of specific heat at constant pressure ( $C_p$ ), relative density ( $\rho$ ), thermal conductivity ( $\lambda$ ) and thermal diffusivity ( $\alpha$ )

as a function of temperature. Using these results, elevated temperature thermal property models are proposed, and comparisons are made to determine the suitable material types/characteristics for use in fire safe building construction.

## **2. Thermal Property Tests**

The thermal properties (specific heat at constant pressure ( $C_p$ ), relative density ( $\rho$ ), thermal conductivity ( $\lambda$ ) and thermal diffusivity ( $\alpha$ )) of the selected building materials representing the commonly used LSF system components were determined using two thermal analysis instruments : simultaneous thermal analysis (STA) - NETZSCH STA 449 F3 Jupiter and laser flash analysis (LFA) - NETZSCH LFA 467 HyperFlash equipment (Table 1). This section presents the essential and specific details of the thermal property test procedures. Further details are given in a related publication by the authors [17].

### **2.1. Specific Heat at Constant Pressure and Relative Density**

Specific heat at constant pressure ( $C_p$ ) and relative density ( $\rho$ ) measurements were obtained using simultaneous thermal analysis (STA) - NETZSCH STA 449 F3 Jupiter (Table 1). Figure 1 shows the principle of STA in which differential scanning calorimetry (DSC) and thermogravimetric analysis (TGA) measurements are taken simultaneously using the same sample. Figure 2 shows the two STA instruments used in this study, STA1: a rhodium furnace that can be heated to 1650°C, STA2: a platinum furnace that can be heated to 1500°C.

In the DSC technique, the heat flow rate to the sample is monitored and compared to a reference material (sapphire standard). Both endothermic (heat flows into a sample) and exothermic (heat flows out of a sample) transitions are measured as a function of temperature. In the TGA technique, the mass of the sample under a controlled temperature program in a specified atmosphere is monitored as a function of temperature or time. This allows simultaneous DSC-TGA measurements of both heat flow and weight change of a sample with respect to temperature or time under controlled atmosphere.

The standard procedures in ASTM E1269 [15] were used in the tests using Platinum (Pt) crucibles lined with Alumina ( $Al_2O_3$ ) liners and Platinum (Pt) pin holed lids (Figure 3). Each test included a defined procedure with three important steps, (1) Baseline measurements (2)

Measurements of Sapphire standard (reference material – 20 mg sapphire disc mass) and (3) Measurements of sample material (initial mass of 20 mg in a powder form). In the case of gypsum plasterboards, the paper layer was removed and only the core material was used. The temperature program for measurements started at 25°C and was then increased to 1200°C at a rate of 20°C/min. Figure 4 illustrates the sapphire discs and the procedure of placing them in the crucible while Figure 5 shows the test photographs of boards, insulation material and plywood. Further details of the above three-step procedure including those of samples are given in [17].

Specific heat and mass loss calculations were conducted using Equations 1 and 2 based on ASTM E1269 [15].

$$C_p(s) = C_p(st) \cdot \frac{D_s \cdot W_{st}}{D_{st} \cdot W_s} \quad (1)$$

where

$C_p(s)$ ,  $C_p(st)$  = specific heat capacity of the sample and sapphire standard ( $J/(g * K)$ ), respectively

$D_s$  = vertical displacement between the sample holder and the sample DSC thermal curves at a given temperature (mW)

$D_{st}$  = vertical displacement between the sample holder and the sapphire DSC thermal curves at a given temperature (mW)

$W_s$ ,  $W_{st}$  = mass of sample and sapphire standard (mg), respectively

$$C_p(actual) = C_p(software) \cdot \frac{1}{mass\ loss} \quad (2)$$

## 2.2. Thermal Conductivity and Thermal Diffusivity

Thermal diffusivity ( $\alpha$  - mm<sup>2</sup>/s) was obtained at elevated temperatures using the laser flash analysis technique [18] adopted in NETZSCH LFA 467 Hyperflash. In the method of determining thermal diffusivity (Figure 6 (a)), the sample front side is heated by a high intensity, short duration light (laser) pulse while an infrared camera records the change of temperature with time on the sample back side. Figure 6 (b) shows a typical temperature versus time curve from which the thermal diffusivity is determined at pre-programmed temperatures. In this study, a heating rate of 20°C/min was used in a purged environment using Nitrogen gas at a rate of 50 ml/min. Thermal diffusivity data were obtained at temperatures from 30 to 500°C at 20°C

intervals, apart from structural plywoods for which the measurements were stopped after 400°C due to their significant mass loss at elevated temperatures and restrictions in supporting the test sample. Three measurements were taken at each temperature to determine the average thermal diffusivity per temperature interval. Specialised sample holders were used to hold either solid or powder samples during testing. Solid square samples of sizes 10 x 10 x 2 mm were used, except for the insulation materials. Insulation materials were made into powders and were tested in the sample holder used in testing liquid metals and powdery samples. Three thin coats of graphite were sprayed on each face of the solid samples, while for the powder samples (insulation materials), the sample holder's sapphire pan bottom surface was sprayed with a cover plate (approx. 10 mm diameter) to ensure that only the outer edges of the pan were coated. Likewise, the underside of the lid was sprayed with the cover plate to ensure that only the inner edges of the lid were coated. In all cases three thin coats of graphite were used. Equation 3 was used in calculating the temperature dependent thermal conductivity,  $\lambda(T)$  in W/m°C, from thermal diffusivity  $\alpha(T)$  in mm<sup>2</sup>/s, specific heat at constant pressure  $C_p$  in J/kg°C, and relative density  $\rho(T)$  in kg/m<sup>3</sup>.

$$\lambda(T) = a(T) \cdot C_p \cdot \rho(T) \quad (3)$$

### 3. Thermal Property Test Results and Discussion

Thermal property measurements as a function of temperature are reported in this section for the 21 materials tested in this study (Table 2). Average results are given for each group of materials investigated, namely, gypsum plasterboards, calcium silicate boards, magnesium oxide boards, perlite boards, insulation materials and structural plywoods.

#### 3.1. Specific Heat at Constant Pressure and Relative Density Measurements

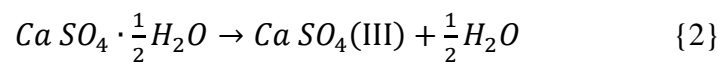
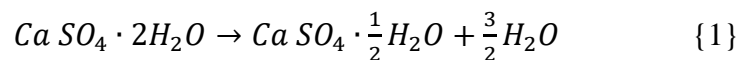
Specific heat and relative density for each material are grouped based on their type and their measured values are reported for temperatures varying in the range of 36 to 1180°C.

##### Gypsum Plasterboards

Figure 7 shows the results of repeated tests conducted to establish reliability of results for each material and to obtain the average results. The average results are shown in this section for each material. Figures 8(a) and (b) show the specific heat at constant pressure and mass loss of

four different commercially available gypsum plasterboards (listed as Boards 1 to 4 in Table 2) while Table 3 gives the descriptions of their chemical compositions. Although they are manufactured by different manufacturers, they exhibit similar and consistent thermal characteristics in relation to the variations of specific heat and mass loss. As seen in Figures 8(a) and (b) the measured thermal properties of the four types of gypsum plasterboards are quite similar despite the different compositions used by their manufacturers (Table 3)

The specific heat values of Gypsum Plasterboards 1 to 4 at the initial temperature are 1108, 1018, 1102 and 1059 Jkg<sup>-1</sup>°C, respectively. They increased rapidly after the temperature of 116°C for all four boards, and the first peak endothermic reaction occurred at 156°C, 160°C, 158°C and 158°C, respectively. At this temperature, the values measured were 12772, 11123, 12346, and 12493 Jkg<sup>-1</sup>°C, respectively. This was followed by a second sudden endothermic reaction at 178°C, 184°C, 182°C and 182°C, respectively, and the values measured were 9991, 9511, 9519 and 10230 Jkg<sup>-1</sup>°C, respectively. Calcium sulphate dihydrate has two water molecules for each calcium sulphate molecule. The chemical reactions that produced the two endothermic decomposition reactions in gypsum plasterboards are caused by the decomposition of calcium sulphate dihydrate being converted back to the powdery material of calcium sulphate hemi-hydrate (chemical reaction {1}). As calcium sulphate hemi-hydrate is heated to higher temperatures, complete de-hydration occurs in a second reaction from calcium sulphate hemi-hydrate (chemical reaction {2}) and results in CaSO<sub>4</sub> (III) - calcium sulphate anhydrite III. This is a high burning process and is known as the complete calcination of gypsum [4].



At higher temperatures, the soluble form of calcium sulphate anhydrite III becomes insoluble in an exothermic reaction at about 400°C. The calcium sulphate anhydrite III transforms to CaSO<sub>4</sub> (II) - calcium sulphate anhydrite II. This is stable up to 1180°C. The final reaction occurs at temperatures higher than 1180°C, where sulphate anhydrite II transforms into a cubic crystal structure of CaSO<sub>4</sub> (I) - calcium sulphate anhydrite I. Magnesium Carbonate (MgCO<sub>3</sub>) and calcium carbonate (CaCO<sub>3</sub>) are the other two possible constituents that can lead to mass loss with subsequent shrinkage and strength loss of commercially available gypsum plasterboards. Decomposition of these carbonates is an endothermic reaction, which takes place at about 770°C for MgCO<sub>3</sub> and 920°C for CaCO<sub>3</sub> (Figure 8 (a)).



Figure 8 (b) shows the mass loss variations for Gypsum Plasterboards 1 to 4. Significant mass loss occurred due to the two endothermic peaks and was in the temperature range of 118 to 184°C, 118 to 188°C, 122 to 192°C and 118 to 202°C for these boards, reaching mass losses of 17%, 16%, 17% and 18%. Further mass loss occurred during the temperature range of 650 to 1180°C, reaching the values of 23%, 23%, 24% and 23%.

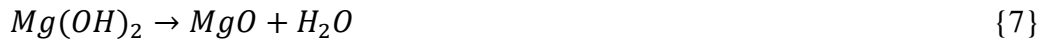
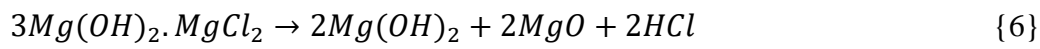
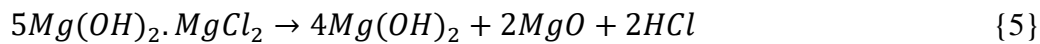
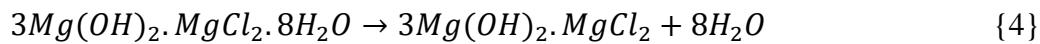
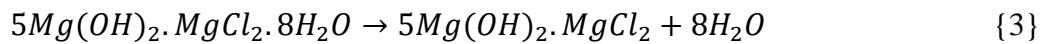
### **Calcium Silicate Boards**

Figure 9 presents the raw data from the STA measurements (DSC, TGA and  $C_p$ ) for Calcium Silicate Board 1 with the details of the sample and test. Figure 10 presents the specific heat and mass loss plots of five commercially available calcium silicate boards while Table 4 gives the descriptions of their chemical compositions. Calcium Silicate Board 1 exhibited similar specific heat and mass loss variations as gypsum plasterboards (see Figure 8) while Calcium Silicate Boards 2, 3 and 4 exhibited a later endothermic reaction. The specific heat values of Calcium Silicate Boards 1 to 5 at the initial temperature were 1085, 873, 915, 908 and 904  $\text{Jkg}^{-1}\text{C}^{-1}$  (Figure 10 (a)). They increased to the values of 12501, 6858, 7170, 9635, 2145  $\text{Jkg}^{-1}\text{C}^{-1}$  at the first peak endothermic reaction, which occurred at 162°C, 798°C, 816°C, 810°C and 744°C for these boards. A second sudden endothermic reaction occurred for Calcium Silicate Board 1 at 186°C with corresponding specific heat value of 10545  $\text{Jkg}^{-1}\text{C}^{-1}$ . The high peaks in Calcium Silicate Board 1 are due to the decomposition of calcium sulphate dihydrate, which were also observed in Gypsum Plasterboards 1 to 4. The later decomposition of Calcium Silicate Boards 2, 3 and 4 is attributed to the presence of xonotlite, which is synthesised during the hydrothermal synthesis process. These calcium silicate boards with xonotlite exhibited the later endothermic decomposition reaction due to the dehydration of xonotlite that occurs at 800°C [19]. This decomposition of xonotlite resulted in a mass loss of 23%, 24% and 31% at 850°C (Figure 10 (b)) for Calcium Silicate Boards 2, 3 and 4, respectively. The mass losses for Calcium Silicate Boards 1 to 5 at 1180°C were 25%, 24%, 25%, 32% and 16%, respectively.

### **Magnesium Oxide Boards**

Figure 11 presents the specific heat and mass loss plots of two commercially available magnesium oxide boards while Table 5 gives their compositions. The specific heats of Magnesium Oxide Boards 1 and 2 at the initial temperature were 1325 and 1183  $\text{Jkg}^{-1}\text{C}^{-1}$ , respectively. They exhibited five chemical reactions related to endothermic peaks as also

reported by Chen et al. [11]. These endothermic reactions occurred for Magnesium Oxide Board 1 at 184°C, 220°C, 374°C, 482°C and 614°C and at these temperatures the values measured were 6503, 6267, 7777, 6748 and 2243 J/kg°C, respectively. For Magnesium Oxide Board 2 the endothermic reactions occurred at 178°C, 234°C, 426°C, 470°C and 626°C and at these temperatures the values measured were 4890, 5816, 6780, 6262 and 1612 J/kg°C, respectively. Chen et al. [11] reported that the first two endothermic peaks of specific heat are caused by the dehydration of magnesium oxychloride cement (chemical reactions {3} and {4}), while the third and fourth peaks (shown by the highest specific heat in both Magnesium Oxide Boards 1 and 2 in Figure 11 (a)) are caused by the hydrolysis of magnesium chloride (chemical reactions {5} and {6}) and the pyrolysis of magnesium hydroxide (chemical reaction {7}), respectively. The fifth endothermic peak in specific heat is caused by the melting of the fibres or decomposition of other materials in magnesium oxide boards.



Significant mass losses occurred (Figure 11 (b)) for Magnesium Oxide Boards when compared with gypsum plasterboards and calcium silicate boards. They were 42% and 44% for Magnesium Oxide Boards 1 and 2, respectively, in the temperature range of 36 to 1180°C.

### Perlite Boards

Figure 12 presents the specific heat and mass loss plots of the two types of Perlite Boards. The specific heat values of Perlite Boards 1 and 2 at the initial temperature were 808 and 921 J/kg°C, respectively. Composition details were not provided by the manufacturers of Perlite Boards. The first endothermic reaction occurred for Perlite Board 1 at 274°C with specific heat value of 1322 J/kg°C. For Perlite Board 2, these values were 328°C and 1963 J/kg°C. A second endothermic reaction occurred at 318°C and the value measured at this temperature was 1444 J/kg°C for Perlite Board 1. At 1180°C, the overall mass losses were 8 and 18% for Perlite Boards 1 and 2, respectively.

## Fire Resistant Boards

Figure 13 compares the specific heat and mass loss plots for all four types of fire resistant boards investigated. In order to delay the heat transfer to the cold-formed steel frames, appropriate selection of fire resistant boards is necessary. Figure 13 (a) shows that Gypsum Plasterboards 1 to 4, Calcium Silicate Boards 1 to 4 and Magnesium Oxide Boards 1 and 2 have higher specific heat values than Perlite boards. The decomposition of these boards requires a substantial amount of energy for the completion of their phase transitions and hence will ideally be suitable for delaying heat transfer to the steel frames in LSF systems. However, Figure 13 (b) shows that Magnesium Oxide Boards have the highest mass loss reduction (42% and 44%) and therefore they will be vulnerable to cracking when fastened to the steel frames. Calcium Silicate Boards 2 to 4 have high specific heat values, but their decomposition occurs at higher temperatures (800°C) when compared with gypsum plasterboards (110 to 220°C). As the standard fire curve will reach 800°C only after 22 min, they must have low thermal conductivity for their suitable application in LSF systems. The lower thermal conductivity will thus prevent a rapid temperature rise before reaching the temperature of 800°C. The thermal conductivity results are presented in the next section.

Gypsum Plasterboard 4, Calcium Silicate Boards 1 and 2 all showed the benefits in terms of high specific heat and low mass loss, in comparison with other boards. Gypsum Plasterboard 4 and Calcium Silicate Board 1 both exhibited high levels of specific heat at lower temperatures. This is important in LSF systems as steel undergoes significant mechanical property reductions at elevated temperatures. Calcium Silicate Board 2 also exhibited high specific heat, but at higher temperatures (800°C). Therefore, further investigations are needed, by evaluating its thermal conductivity (Section 3.2).

## Insulation Materials

Figure 14 presents the specific heat and mass loss plots of six commercially available insulation materials, Glass Fibre, Rockwool Fibre, Cellulose Fibre, Aerogel Insulation 1, 2 and 3. Table 6 gives the compositions of these insulation materials. The specific heats of these insulation materials at the initial temperature are 917, 865, 1094, 743, 607 and 697 J/kg°C, respectively. Figure 14 (a) shows a highly exothermic reaction with no associated mass change in Rockwool fibre after 900°C. This exothermic reaction is due to the crystallization of

rockwool fibres while the following endothermic reaction after 1000°C identifies the melting of rockwool fibres. Cellulose fibre has the highest specific heat due to the decomposition of boric acid at relatively lower temperatures. This is ideal for use in LSF systems as an insulation material with high specific heat, although cellulose has a significantly high mass loss compared with other insulation materials (Figure 14 (b)). In the full temperature range of 36 to 1180°C, the mass losses were 5%, 3%, 59%, 6%, 6% and 5%, respectively, i.e. the negligible mass loss except for cellulose fibre (59%). Figures 15 (a) and (b) show the glass transition temperatures of 576.0°C and 683.1°C for glass fibre and rockwool fibre, respectively. Therefore, after the glass transition the insulation material may become less effective in preventing the heat transfer through the LSF system.

### **Structural Plywoods**

Figure 16 shows the specific heat values of structural plywoods F8 Stress Grade and F11 Stress Grade. The specific heats of these plywoods at the initial temperature were 1213 and 1187 J/kg°C, respectively. Plywood will not ignite below a critical surface temperature. When the surface temperature increases above 100°C volatile gases begin to be emitted as thermal degradation slowly commences. Specific heat increased to the first endothermic peak at a temperature of 122°C for both F8 and F11 structural plywoods. At this temperature, the values measured were 2048 and 2045 J/kg°C, respectively. However, it is not until the temperature in excess of 200°C that there is a sufficient build-up of these gases to cause the ignition of plywood. Plywood undergoes a sudden endothermic decomposition as indicated by charring of the wood surface and mass loss. This is shown in Figure 16 with the average specific heat for the second endothermic peak occurring at a temperature of 206 and 234°C. At these temperatures, the average values were 1708 and 1773 J/kg°C. Heating plywood above 200°C causes decomposition or pyrolysis converting it to gases, tar and charcoal. Plywood undergoes an exothermic reaction (burning) as evident from a significant mass loss (Figure 16 (b)).

Above these temperatures the gases will cause plywood to vigorously burn until 434 (F8 stress grade) and 438°C (F11 stress grade) whereby plywood becomes charcoal. At these temperatures, the average values were -574 and -739 J/kg°C. Charcoal then exhibits the second endothermic peak at 676°C and 672°C, respectively. At this point, the measured values were 2705, and 1963 J/kg°C, respectively. Significant mass losses of 70 and 72% occurred for the two structural plywoods.

### **3.2. Thermal Conductivity and Thermal Diffusivity Measurements**

Laser flash analysis (NETZSCH LFA 467) was used in the measurements of thermal diffusivity in this study. Thermal diffusivity was not measured beyond 500°C because of the equipment limitations while the tests were stopped after 400°C for structural plywoods due to the significant mass loss (Figure 16 (b)). Average results of thermal diffusivity and thermal conductivity were determined by conducting multiple tests for each material. Material densities were measured (Table 2) and used in thermal conductivity calculations based on Equation 3.

#### **Gypsum Plasterboard**

Figure 17 presents the thermal diffusivity measurements and thermal conductivity calculated using Equation 3 for Gypsum Plasterboard 4. The thermal conductivity reduces in stages from 30 to 500°C (0.269 to 0.129 W/m/°C). It reduces significantly from 0.237 to 0.185 W/m/°C in the temperature range of 80 to 100°C. However, it increases from 0.119 to 0.129 W/m/°C when the temperature is increased from 340 to 500°C. The thermal conductivity values of Gypsum Plasterboards 1 to 3 were measured by another researcher in the authors' group [7] and they are plotted together with those of Gypsum Plasterboard 4 in Figure 18.

#### **Calcium Silicate Boards**

Figure 19 shows the raw data obtained from LFA measurements for Calcium Silicate Board 1. Figure 19 (b) shows a very good agreement with measured (blue line) temperature versus time curves with calculated model (red line) for thermal diffusivity, highlighting the confidence in the measured results. Figures 20(a) and (b) present the measured thermal diffusivity and thermal conductivity values for Calcium Silicate Boards 1 to 5. Figure 20 (b) shows the significant differences among them due to their chemical composition differences. Calcium Silicate Board 1 resembles the thermal conductivity of gypsum plasterboards with a similar reduction in thermal conductivity from 100°C to 120°C and an increase after 340°C. Calcium Silicate Boards 2 and 3 have the lowest thermal conductivities of all the boards tested, which remain almost constant for the temperature range of 30 to 500°C (0.087 to 0.072 W/m/°C for Calcium Silicate Board 2 and 0.115 to 0.093 W/m/°C for Calcium Silicate Board 3). Calcium Silicate Boards 4 and 5 have the highest thermal conductivity values with almost a linear relationship from 30 to 500°C (0.524 to 0.338 and 0.422 to 0.268 W/m/°C).

## **Magnesium Oxide Board**

Figure 21 shows the thermal diffusivity and thermal conductivity values for Magnesium Oxide Boards 1 and 2. The thermal conductivity values are almost the same for these boards and reduce linearly with increasing temperature from 30°C to 500°C (0.424 to 0.141 and 0.432 to 0.123 W/m/°C).

## **Perlite Board**

Figure 22 presents the thermal diffusivity and thermal conductivity values for Perlite Boards 1 and 2. The thermal conductivity and density of perlite boards are the lowest of all board materials tested and their thermal conductivity increases linearly in the temperature range of 30 to 500°C (0.049 to 0.064 and 0.064 to 0.082 W/m/°C).

## **Fire Resistance Boards**

Figure 23 compares the thermal conductivity values of all the fire resistant boards. Both Perlite Boards and Calcium Silicate Boards 2 and 3 have the lowest thermal conductivity values. They remain relatively constant for the entire temperature range of 30 to 500°C. However, perlite boards do not exhibit high specific heat properties and therefore their thickness need to be increased in order to delay the heat transfer and to be a suitable alternative. Low density calcium silicates boards (Calcium Silicates Boards 2 and 3) have very low thermal conductivity despite later decomposition and are therefore recommended for use as face layer boards in order to provide higher fire resistance levels (FRLs). Gypsum plasterboards and Calcium Silicate Board 1 perform relatively similarly. Calcium Silicate Board 4 has the highest specific heat at 800°C and is therefore suitable in applications where the FRL requirements are based on the hydrocarbon fire curve (800°C within 2 min).

## **Insulation Materials**

Figure 24 presents the thermal diffusivity and thermal conductivity values for glass fibre, rockwool fibre and cellulose fibre. Aerogel Insulations 1, 2 and 3 could not be tested due to the limitation of the Laser Flash instrument for very low conductivity materials. The thermal conductivities of glass fibre and rockwool fibre are almost uniform in the temperature range of

30 to 500°C (0.018 to 0.011 W/m/°C for rockwool and 0.036 to 0.034 W/m/°C for glass fibre). Cellulose fibre has a sudden increase in thermal conductivity almost instantly, then reduces after 100 to 120°C and increases again after 260°C.

### **Structural Plywoods**

Figure 25 presents the thermal diffusivity and thermal conductivity values for Plywoods F8 and F11 Stress Grades. The temperature was limited to 400°C due to the significant mass loss of wood and the issues relating to supporting the plywood samples in the sample holder. The thermal conductivity values of Plywoods F8 and F11 Stress Grades vary almost linearly from 30 to 400°C (0.122 to 0.058 and 0.122 and 0.065 W/m/°C).

### **3.3. Benchmark Study Using Results from Other Studies**

This section compares the thermal property results from this study with similar results from other studies to demonstrate the accuracy of our results before proposing suitable predictive equations. However, comparisons with most of the thermal property results from other studies were not possible because of the following reasons related to the results from other studies: (1) they are often manufacturers' data for ambient temperature only (2) elevated temperature thermal property data of boards and insulation materials are not available, except for some boards (3) even when some elevated temperature data are available, there are differences in the test methods such as the use of non-standard test method and different heating rates (4) tested boards appear to have different compositions although given the same generic name. However, comparisons have been made with some elevated temperature thermal property data as shown in Figures 8 and 18 for gypsum plasterboards and Figures 11 and 21 for magnesium oxide boards. Comparisons with the gypsum plasterboard results from Dodangoda et al. [7] (Figures 8 and 18) show a good agreement. In the comparisons with the magnesium oxide board results from Chen et al. [11] (Figures 11 and 21), there are some differences, which are likely to be due to the differences in the chemical composition of magnesium oxide boards and the test methods used (specific heat measurements at a heating rate of 5°C/min). However, overall agreement exhibited in these figures gives confidence to the accuracy of the thermal property results reported in this paper.

#### **4. Proposed Thermal Property Equations for Numerical Modelling**

This section proposes suitable predictive equations for specific heat, relative density and thermal conductivity of the tested materials based on the average measured thermal property results, which can be used in numerical models to predict the heat transfer in LSF systems. Specific heat equations are proposed for the temperature range of 36 to 1180°C, while thermal conductivity equations are proposed for the temperature range of 30 to 500°C. The proposed equations are given in Table 7 for Gypsum Plasterboard 4, Calcium Silicate Board 1, Calcium Silicate Board 2, Perlite Board 1, Rockwool Fibre Insulation and Plywood F11 Stress Grade, respectively. These boards and insulation were chosen mostly because of their better thermal characteristics that have the potential to enhance the FRL of LSF systems. Suitable fire resistant boards are chosen and used in LSF systems if they exhibit high specific heat, low thermal conductivity, reduced mass loss and low bulk density.

There was hardly any difference among the four types of gypsum plasterboard tested in this investigation as seen in Fig. 8. Gypsum Plasterboard 4 was chosen due to its high specific heat at lower temperatures and low mass loss for temperatures up to 1200°C. Similar behaviour was also found for Calcium Silicate Board 1. Calcium Silicate Board 2 was chosen based on its low thermal conductivity and high specific heat values, while Perlite Board 1 was chosen due to its low bulk density and low thermal conductivity values at temperatures up to 500°C. Rockwool fibre Insulation was chosen due to its lower thermal conductivity in comparison with glass fibre and cellulose fibre insulations. Plywood F11 Stress Grade was chosen based on its common usage in conventional LSF floor-ceiling systems with 600 mm joist spacing.

Figures 26 to 31 compare the predicted values of specific heat, relative density and thermal conductivity based on the proposed equations with the corresponding measured average values, which demonstrate a good agreement between them.

#### **5. Conclusions**

This paper has presented the details of a series of elevated temperature thermal property tests of a set of commercially available component materials used in the construction of LSF systems. This experimental study included gypsum plasterboards, calcium silicate boards, magnesium oxide boards, perlite boards, insulation materials and structural plywoods, totalling 21 LSF



components. Tests were conducted based on ASTM standard test methods and the results of specific heat at constant pressure, relative density, thermal conductivity and thermal diffusivity are given as a function of temperature for each material. Commercially available gypsum plasterboards had similar elevated temperature thermal properties despite the differences in their compositions. It was found that Gypsum Plasterboards 1 to 4, Calcium Silicate Boards 1 to 4 and Magnesium Oxide Boards 1 and 2 had higher specific heat values than Perlite boards. The decomposition of these boards requires a substantial amount of energy for the completion of their phase transitions and hence were identified as suitable for delaying the heat transfer to the steel frames in LSF systems. However, it was found that Magnesium Oxide Boards have the highest mass loss (42 and 44%) among all the fire resistant boards, therefore they will be vulnerable to cracking and integrity failures when fastened to the steel frames. Low density calcium silicate boards with xonotlite were found to be superior in regard to thermal conductivity although their decomposition occurred later at temperatures around 800°C. Structural plywoods of two different stress grades considered in this research had negligible differences in relation to their thermal characteristics. It was found that structural plywood undergoes decomposition at relatively low temperatures with combustion occurring at temperatures above 234°C, resulting in vigorous burning of the wood with significant mass loss of about 70%.

New thermal property models of specific heat, relative density and thermal conductivity are proposed for Gypsum Plasterboard 4, Calcium Silicate Board 1, Calcium Silicate Board 2, Perlite Board 1, Rockwool Fibre Insulation and Plywood F11 Stress Grade to advance their use in improved fire rated LSF systems. Except for plywood, they were chosen due to their superior characteristics of high specific heat, low thermal conductivity, reduced mass loss and low bulk density when compared with other materials.

This advanced knowledge and understanding of the elevated temperature thermal properties of a range of commonly used building materials as presented in this paper allows accurate prediction of the fire resistance of LSF systems constructed of such materials using appropriate numerical and fire design methods and facilitate the development of improved LSF systems with enhanced FRL.

## Acknowledgments



The authors would like to thank Australian Research Council for their financial support (DE150101104 and DP160102879), and the Queensland University of Technology for providing the necessary facilities and support to conduct this research project. They wish to thank Dr Keerthan Poologanathan for his advice and support to the first author during the early stages of his PhD project. They would also like to thank Ms. Elizabeth Graham at the Central Analytical Research Facility hosted by the Institute for Future Environments at QUT for her valuable assistance in performing the thermal property tests.

## References

- [1] Park, S. H., Manzello, S. L., Bentz, D. P. and Mizukami, T. 2009. Determining thermal properties of gypsum board at elevated temperatures. *Fire and Materials*. Vol. 34: pp. 237-250.
- [2] Keerthan, P. and Mahendran, M. 2012a. Numerical studies of gypsum plasterboard panels under standard fire conditions. *Fire Safety Journal*. Vol. 53: pp. 105-119.
- [3] Keerthan, P. and Mahendran, M. 2012b. Numerical modelling of non-load-bearing light gauge cold-formed steel frame walls under fire conditions. *Journal of Fire Sciences*. Vol. 30: pp. 375-403.
- [4] Singh, N. B. and Middendorf, B. 2007. Calcium sulphate hemihydrate hydration leading to gypsum crystallization. *Progress in Crystal Growth and Characterization of Materials*. Vol. 53: pp. 57-77.
- [5] Thomas, G. 2002. Thermal properties of gypsum plasterboard at high temperatures. *Fire and Materials*. Vol. 26: pp. 37-45.
- [6] Bénichou, N. and Sultan, M. A. 2005. Thermal Properties of Lightweight-Framed Construction Components at Elevated Temperatures. *Fire and Materials*. Vol. 29: pp. 165-179.
- [7] Dodangoda, M. T., Mahendran, M., Keerthan, P. and Frost, R. L. 2019. Developing a performance factor for fire rated boards used in LSF wall systems. *Fire Safety Journal*. Vol. 109: pp. 1-13.
- [8] Anton, O., Jacops, J. and Opsommer, A. 2003. Gypsum Based Material, Method for Making Same and Fire Protection Building Element Comprising Same. European Patent EP1062184A1, Filed December 17, 2000, and Issued August 20, 2003.

- [9] Do, C. T., Bentz, D. P. and Stutzman, P. E. 2007. Microstructure and Thermal Conductivity of Hydrated Calcium Silicate Board Materials. *Journal of Building Physics*. Vol. 31: pp. 55-67.
- [10] Promat. 2014. Promat Calcium Silicate Insulation, Accessed May 23, 2018. <https://www.promat-hpi.com/en/downloads>.
- [11] Chen, W., Ye, J., Bai, Y. and Zhao, X. 2014. Thermal and Mechanical Modeling of Load-Bearing Cold-Formed Steel Wall Systems in Fire. *Journal of Structural Engineering*. Vol. 140: pp. 1-13.
- [12] Baetens, R., Jelle, B. P. and Gustavsen, A. 2011. Aerogel Insulation for Building Applications: A State-of-the-Art Review. *Energy and Buildings*. Vol. 43: pp. 761-769.
- [13] EWPA. 2018a. Structural Plywood and LVL. <http://ewp.asn.au/wp-content/uploads/2018/12/EWPA-Structural-Plywood-LVL-Design-Guide-v5-FINAL-1.pdf>.
- [14] EWPA. 2018b. Fire Performance. <http://ewp.asn.au/wp-content/uploads/2018/10/Fact-Sheet-Fire-Performance-Fact-Sheet-v7-FINAL.pdf>.
- [15] ASTM E1269. 2018. Standard Test Method for Determining Specific Heat Capacity by Differential Scanning Calorimetry. ASTM International. West Conshohocken, PA, USA.
- [16] ASTM E1461. 2013. Standard Test Method for Thermal Diffusivity by the Flash Method. ASTM International. West Conshohocken, PA, USA.
- [17] Steau, E., Mahendran, M. and Poologanathan, K. (2020) Elevated temperature thermal properties of carbon steels used in cold-formed light gauge steel frame systems, *Journal of Building Engineering*, Vol. 28, 101074.
- [18] Parker, W. J., Jenkins, R.J., Butler, C.P. and Abbott, G.L. 1961, Flash method of determining thermal diffusivity, heat capacity, and thermal conductivity, *Journal of Applied Physics*. Vol. 32, pp. 1679-1684.
- [19] Dent, L. S. and Taylor, H. F. W. 1956. The Dehydration of Xonotlite. *Acta Crystallographica*. Vol. 9: pp. 1002-1004.

**Table 1: Thermal Analysis Instruments**

Instrument	Thermal Analysis	Thermal Property	Instrument	Technical Specifications
NETZSCH STA 449 F3 <i>Jupiter</i>	Differential Scanning Calorimetry (DSC)  Thermogravimetric Analysis (TGA)	Specific Heat at Constant Pressure ( $C_p$ )  Relative Density ( $\rho$ ) / Mass Loss		DSC resolution: $1\mu\text{W}$ for DSC sensor Type S  Temperature resolution: 0.001 K  Balance resolution: 0.1 $\mu\text{g}$
NETZSCH LFA 467 <i>HyperFlash</i>	Laser Flash Analysis (LFA)	Thermal Conductivity ( $\lambda$ )  Thermal Diffusivity ( $\alpha$ )		Accuracy (Thermal Diffusivity): $\pm 3\%$  Repeatability (Thermal Diffusivity): $\pm 2\%$

**Table 2: Description of Tested Building Materials**

Product	Material	Property Tested	Density (kg/m <sup>3</sup> )
Gypsum	Gypsum Plasterboard 1 <sup>A</sup>	$C_p$ and $\rho$	813
Gypsum	Gypsum Plasterboard 2 <sup>B</sup>	$C_p$ and $\rho$	788
Gypsum	Gypsum Plasterboard 3 <sup>C</sup>	$C_p$ and $\rho$	785
Gypsum	Gypsum Plasterboard 4 <sup>D</sup>	$C_p$ , $\lambda$ , $\rho$ and $\alpha$	836
Calcium Silicate	Calcium Silicate Board 1 <sup>E</sup>	$C_p$ , $\lambda$ , $\rho$ and $\alpha$	875
Calcium Silicate	Calcium Silicate Board 2 <sup>E</sup>	$C_p$ , $\lambda$ , $\rho$ and $\alpha$	450
Calcium Silicate	Calcium Silicate Board 3 <sup>E</sup>	$C_p$ , $\lambda$ , $\rho$ and $\alpha$	568
Calcium Silicate	Calcium Silicate Board 4 <sup>E</sup>	$C_p$ , $\lambda$ , $\rho$ and $\alpha$	1729
Calcium Silicate	Calcium Silicate Board 5 <sup>E</sup>	$C_p$ , $\lambda$ , $\rho$ and $\alpha$	1093
Magnesium Oxide	Magnesium Oxide Board 1 <sup>E</sup>	$C_p$ , $\lambda$ , $\rho$ and $\alpha$	1100
Magnesium Oxide	Magnesium Oxide Board 2 <sup>E</sup>	$C_p$ , $\lambda$ , $\rho$ and $\alpha$	1100
Perlite	Perlite Board 1 <sup>F</sup>	$C_p$ , $\lambda$ , $\rho$ and $\alpha$	204
Perlite	Perlite Board 2 <sup>G</sup>	$C_p$ , $\lambda$ , $\rho$ and $\alpha$	277
Insulation	Glass Fibre Insulation	$C_p$ , $\lambda$ , $\rho$ and $\alpha$	11
Insulation	Rockwool Fibre Insulation	$C_p$ , $\lambda$ , $\rho$ and $\alpha$	100
Insulation	Cellulose Fibre Insulation	$C_p$ , $\lambda$ , $\rho$ and $\alpha$	125
Insulation	Aerogel Insulation 1	$C_p$ and $\rho$	176
Insulation	Aerogel Insulation 2	$C_p$ and $\rho$	176
Insulation	Aerogel Insulation 3	$C_p$ and $\rho$	176
Wood	Plywood F8 Stress Grade	$C_p$ , $\lambda$ , $\rho$ and $\alpha$	550
Wood	Plywood F11 Stress Grade	$C_p$ , $\lambda$ , $\rho$ and $\alpha$	550

Note: Specific heat at constant pressure ( $C_p$ ), thermal conductivity ( $\lambda$ ), relative density ( $\rho$ ) and thermal diffusivity ( $\alpha$ )

<sup>A to G</sup> Boards were obtained from different manufacturers

**Table 3: Compositions of Gypsum Plasterboards**

No.	Ingredients (%)													
	Calcium Sulphate Dihydrate (Gypsum)	Clay	Fly Ash	Vermiculite	Starch	Glass Fibres	Quartz (Crystalline Silica)	Paraffin Wax	Cellulose	Triethanolamine	Sucrose	Siloxane	Boric Acid	Additive(s)
1	>60	1-10	1-10	1-10	1-5	0-2	0.3-0.9							
2	>80		<10	<5	<1	<1	<1		<5	<0.01	<1			<1
3	>95	0-33		0-4	<1			0-6	<1					
4	>70			>4	<3	<1	<0.1	>2	<15			<1	<0.5	

**Table 4: Compositions of Calcium Silicate Boards**

Calcium Silicate Board	Ingredients (%)								
	Calcium Silicate	Quartz (Crystalline Silica)	Portland Cement	Cellulose	Sand, Amorphous	Glass Fibres	Filler(s)	Binding Agent	Additive(s)
1	>60	<1						6-30	Remainder
2	>60	<1		<10		<10			
3	<90	<1						<6	Remainder
4			5-50	5-50					
5	15-25		15-25	<10	15-25		<40		

**Table 5: Compositions of Magnesium Oxide Boards**

Magnesium Oxide Board	Ingredients (%)							
	Magnesium Oxide	Sorel Cement	Perlite	Glass Fibre	Glass Oxide	Wood	Water	Non-Hazardous Ingredients
1		N.A.	N.A.	N.A.		N.A.	N.A.	
2	>60		<10		<5	<5	<15	<5



**Table 6: Compositions of Insulations**

Ingredients (%)								
Insulation	Biosoluble Glass Mineral Wool	Biosoluble Rock	Cellulose Fibre	Thermo Set Inert Polymer	Mineral Oil	Silicone Oil	Boric Acid	
Glass Fibre	87-100			0-13				
Rockwool		>95-99		≤5	≤0.3	≤0.5		
Cellulose			>83					>11.2
Ingredients (%)								
Aerogel	Silica Amorphous, Fumed, Hydrophobic	Fibrous Glass (Textile Grade)	Titanium Dioxide	Alumina Hydrate	Magnesium Hydroxide	Ferric Oxide	Pigment Proprietary	Non-Hazardous Ingredients
1	40-55	40-50	1-6	0-5	0-5		0-1	
2	40-50	40-50		1-5		1-5		<10
3	40-55	40-55	1-5	<5				

**Table 7: Proposed Thermal Property Equations**

Specific heat at constant pressure ( $C_p$ ) in J/kg°C			Relative density ( $\rho$ ) in %			Thermal conductivity ( $\lambda$ ) in W/m°C		
Gypsum Plasterboard 4	$36 \leq T \leq 110^\circ\text{C}$	1059 (4a)	$36 \leq T \leq 120^\circ\text{C}$	100 (5a)	$30 \leq T \leq 80^\circ\text{C}$	$-0.00064T + 0.28855$ (6a)		
	$110 < T \leq 158^\circ\text{C}$	$238.21T - 25144$ (4b)	$120 < T \leq 190^\circ\text{C}$	$-0.2429T + 129.14$ (5b)	$80 < T \leq 100^\circ\text{C}$	$-0.00262T + 0.44648$ (6b)		
	$158 < T \leq 174^\circ\text{C}$	$-161.125T + 37951$ (4c)	$190 < T \leq 700^\circ\text{C}$	$-0.0039T + 83.745$ (5c)	$100 < T \leq 120^\circ\text{C}$	$-0.00036T + 0.22071$ (6c)		
	$174 < T \leq 182^\circ\text{C}$	$39.375T + 3063.8$ (4d)	$700 < T \leq 1180^\circ\text{C}$	$-0.0083T + 86.833$ (5d)	$120 < T \leq 160^\circ\text{C}$	$-0.00079T + 0.27178$ (6d)		
	$182 < T \leq 220^\circ\text{C}$	$-241.34T + 54154$ (4e)			$160 < T \leq 340^\circ\text{C}$	$-0.00015T + 0.17018$ (6e)		
	$220 < T \leq 1180^\circ\text{C}$	1059 (4f)			$340 < T \leq 500^\circ\text{C}$	$0.000064T + 0.097228$ (6f)		
Calcium Silicate Board 1	$36 \leq T \leq 110^\circ\text{C}$	1085 (7a)	$36 \leq T \leq 130^\circ\text{C}$ :	100 (8a)	$30 \leq T \leq 100^\circ\text{C}$	$-0.000814T + 0.34257$ (9a)		
	$110 < T \leq 162^\circ\text{C}$	$219.54T - 23064$ (7b)	$130 < T \leq 190^\circ\text{C}$ :	$-0.2833T + 136.83$ (8b)	$100 < T \leq 120^\circ\text{C}$	$-0.00233T + 0.49443$ (9b)		
	$162 < T \leq 176^\circ\text{C}$	$-166.286T + 39439$ (7c)	$190 < T \leq 800^\circ\text{C}$ :	$-0.0033T + 83.623$ (8c)	$120 < T \leq 140^\circ\text{C}$	$0.000842T + 0.113518$ (9c)		
	$176 < T \leq 186^\circ\text{C}$	$37.2T + 3625.8$ (7d)	$800 < T \leq 1180^\circ\text{C}$ :	$-0.0158T + 93.632$ (8d)	$140 < T \leq 240^\circ\text{C}$	$-0.00075T + 0.33624$ (9d)		
	$186 < T \leq 220^\circ\text{C}$	$-278.235T + 62297$ (7e)			$240 < T \leq 340^\circ\text{C}$	$-0.000283T + 0.224221$ (9e)		
	$220 < T \leq 1180^\circ\text{C}$ :	1085 (7f)			$340 < T \leq 500^\circ\text{C}$	$0.000137T + 0.081646$ (9f)		
Calcium Silicate Board 2	$36 \leq T \leq 70^\circ\text{C}$	873 (10a)	$36 \leq T \leq 650^\circ\text{C}$ :	$-0.0114T + 100.41$ (11a)	$30 \leq T \leq 500^\circ\text{C}$ :	$-0.00005T + 0.0921$ (12)		
	$70 < T \leq 150^\circ\text{C}$	$9.6T + 201$ (10b)	$650 < T \leq 750^\circ\text{C}$ :	$-0.07T + 138.5$ (11b)				
	$150 < T \leq 300^\circ\text{C}$	$-4.0333T + 2246$ (10c)	$750 < T \leq 820^\circ\text{C}$ :	$-0.1286T + 182.43$ (11c)				
	$300 < T \leq 600^\circ\text{C}$	$1.24T + 664$ (10d)	$820 < T \leq 1180^\circ\text{C}$ :	$-0.0028T + 79.278$ (11d)				
	$600 < T \leq 750^\circ\text{C}$	$12.447T - 6060$ (10e)						
	$750 < T \leq 798^\circ\text{C}$	$74.6458T - 52709$ (10f)						
	$798 < T \leq 830^\circ\text{C}$	$-204.9375T + 170398$ (10g)						
	$830 < T \leq 1180^\circ\text{C}$	300 (10h)						
Perlite Board 1	$36 \leq T \leq 200^\circ\text{C}$	$2.4451T + 719.98$ (13a)	$36 \leq T \leq 290^\circ\text{C}$ :	$-0.0039T + 100.14$ (14a)	$30 \leq T \leq 500^\circ\text{C}$ :	$0.00003T + 0.0467$ (15)		
	$200 < T \leq 290^\circ\text{C}$	$1.2444T + 960.11$ (13b)	$290 < T \leq 350^\circ\text{C}$ :	$-0.0833T + 123.17$ (14b)				
	$290 < T \leq 320^\circ\text{C}$	$4.1T + 132$ (13c)	$350 < T \leq 1180^\circ\text{C}$ :	$-0.0024T + 94.843$ (14c)				
	$320 < T \leq 380^\circ\text{C}$	$-5.7333T + 3278.7$ (13d)						
	$380 < T \leq 700^\circ\text{C}$	$-0.525T + 1299.5$ (13e)						
	$700 < T \leq 1180^\circ\text{C}$	$0.4542T + 614.08$ (13f)						
Rockwool Fibre Insulation	$36 \leq T \leq 660^\circ\text{C}$	$0.1538T + 859.46$ (16a)	$36 \leq T \leq 1180^\circ\text{C}$ :	$-0.0026T + 100.09$ (17)	$30 \leq T \leq 500^\circ\text{C}$ :	$-0.000015T + 0.018447$ (18)		
	$660 < T \leq 700^\circ\text{C}$	$12.15T - 7058$ (16b)						
	$700 < T \leq 1180^\circ\text{C}$	1447 (16c)						
Plywood F11 Stress Grade	$36 \leq T \leq 70^\circ\text{C}$	$6.5882T + 949.82$ (19a)	$36 \leq T \leq 220^\circ\text{C}$ :	$-0.0054T + 100.2$ (20a)	$30 \leq T \leq 400^\circ\text{C}$ :	$-0.00016T + 0.12829$ (21)		
	$70 < T \leq 122^\circ\text{C}$	$12.192T + 557.54$ (19b)	$220 < T \leq 290^\circ\text{C}$ :	$-0.0714T + 114.71$ (20b)				
	$122 < T \leq 172^\circ\text{C}$	$-7.9T + 3008.8$ (19c)	$290 < T \leq 400^\circ\text{C}$ :	$-0.4818T + 233.73$ (20c)				
	$172 < T \leq 234^\circ\text{C}$	$1.9839T + 1308.8$ (19d)	$400 < T \leq 500^\circ\text{C}$ :	$-0.07T + 69$ (20d)				
	$234 < T \leq 260^\circ\text{C}$	$-4.3077T + 2781$ (19e)	$500 < T \leq 600^\circ\text{C}$ :	$-0.03T + 49$ (20e)				
	$260 < T \leq 382^\circ\text{C}$	$-13.295T + 5117.7$ (19f)	$600 < T \leq 1180^\circ\text{C}$ :	$-0.0052T + 34.103$ (20f)				
	$382 < T \leq 1180^\circ\text{C}$	39 (19g)						

Note: T is the board temperature ( $^\circ\text{C}$ ).

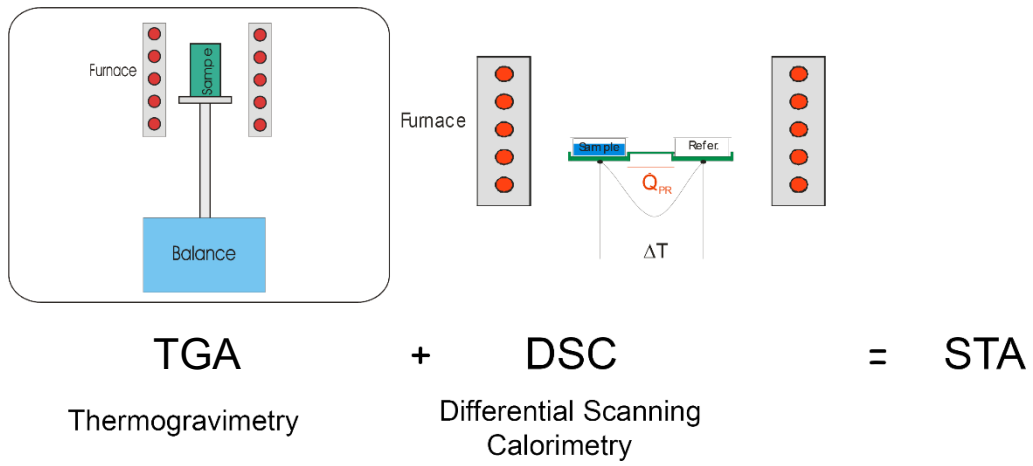
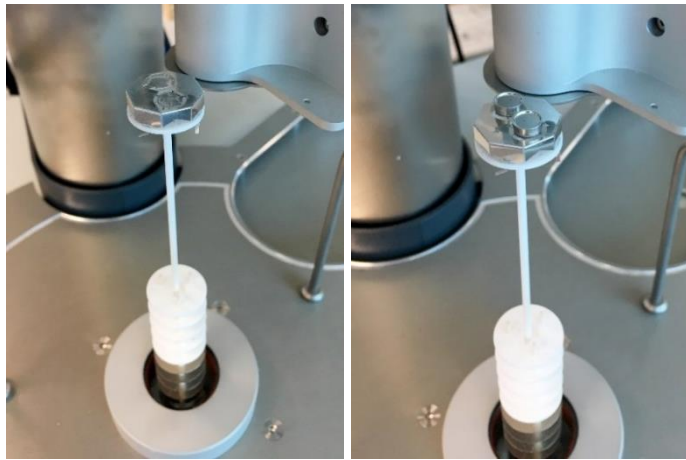


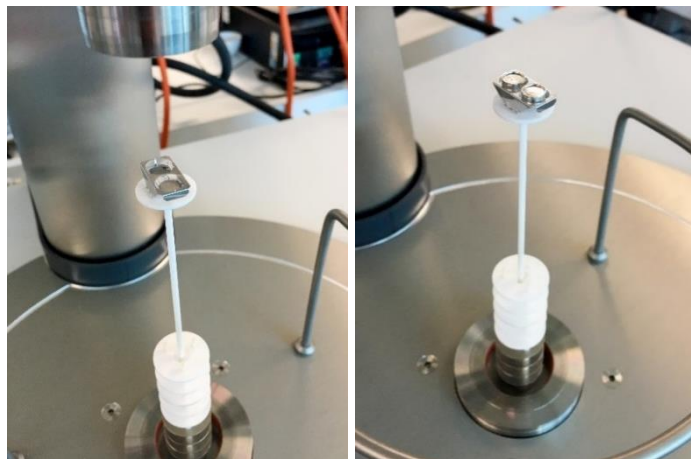
**Figure 1: Differential Scanning Calorimetry (DSC) and Thermogravimetric Analysis (TGA)**



(a) NETZSCH STA 449 F3 Jupiter



(b) STA1 sample holder with and without crucibles



(c) STA2 sample holder with and without crucibles

**Figure 2: NETZSCH STA 449 F3 Jupiter Instrument and Sample Holders**



**Figure 3: Platinum Crucibles Lined with Alumina Liners and Pin Holed Lids**

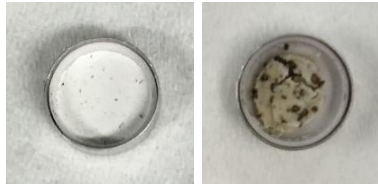


(a) Different sizes of sapphire discs supplied by NETZSCH



(b) 0.25 mm (20.6 mg and 20.9 mg) sapphire disc placed in the crucible

**Figure 4: Sapphire Disc (Reference Material)**



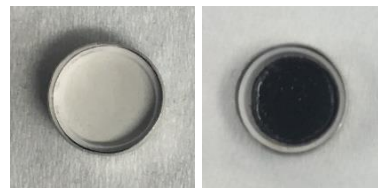
(a) Gypsum Plasterboard 4



(b) Calcium Silicate Board 1



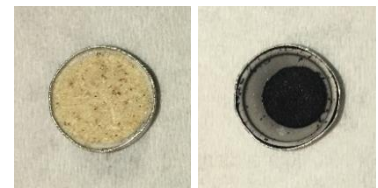
(c) Calcium Silicate Board 2



(d) Perlite Board 1

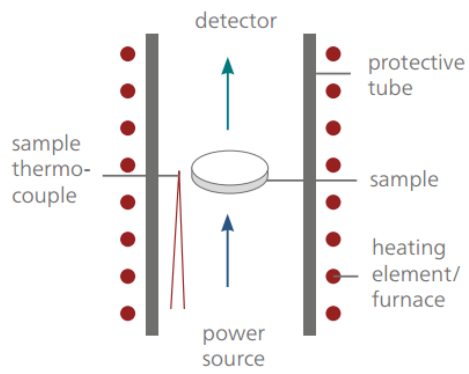


(e) Rockwool Fibre Insulation



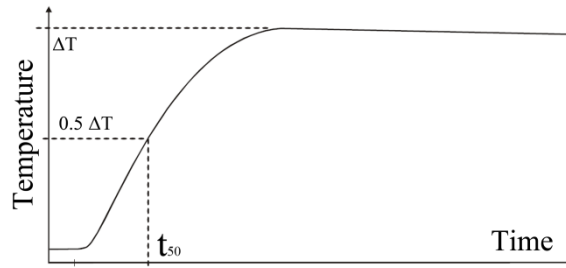
(f) Plywood F11 Stress Grade

**Figure 5: Test Samples Before (Left) and After (Right) Test**

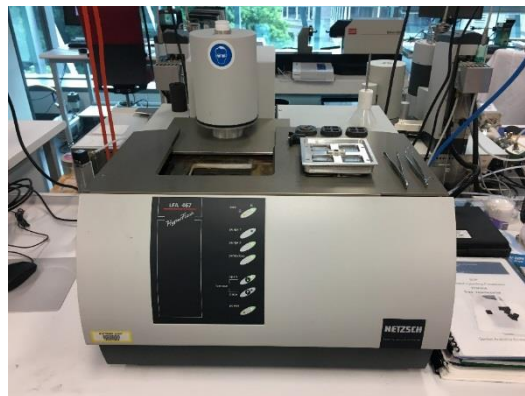


Flash Technique

(a) Principle



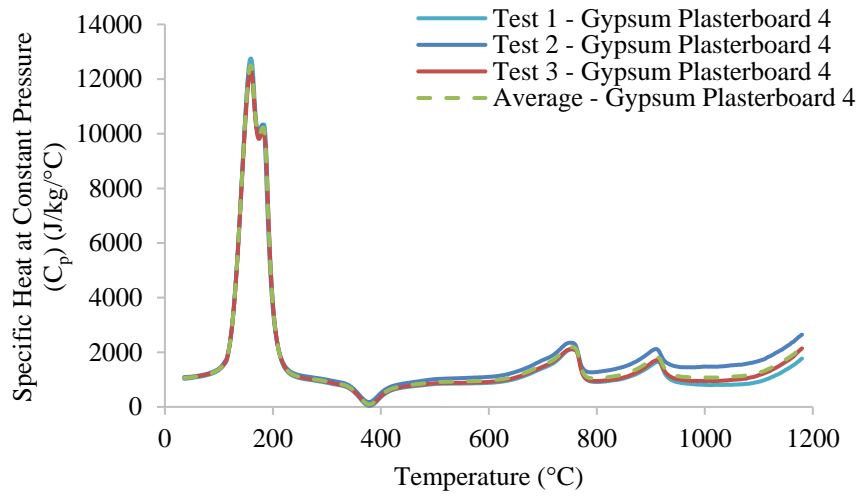
(b) Typical temperature versus time curve



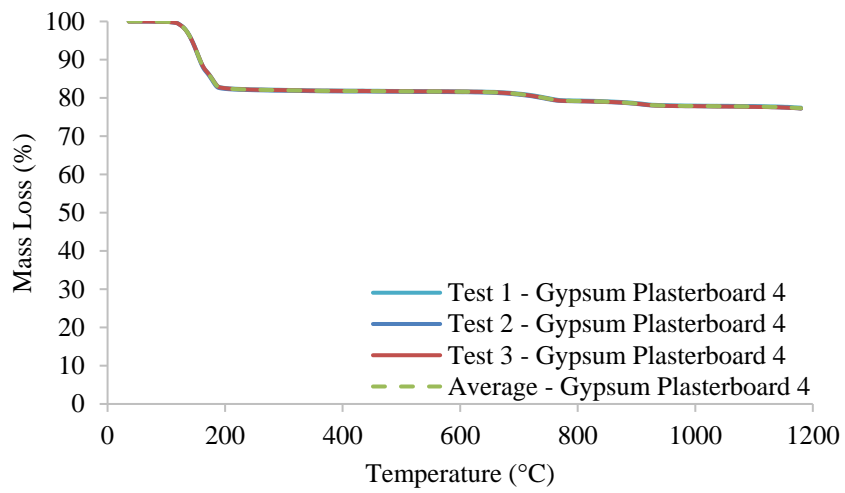
(c) NETZSCH LFA 467 Hyperflash Instrument

**Figure 6: Laser Flash Method**



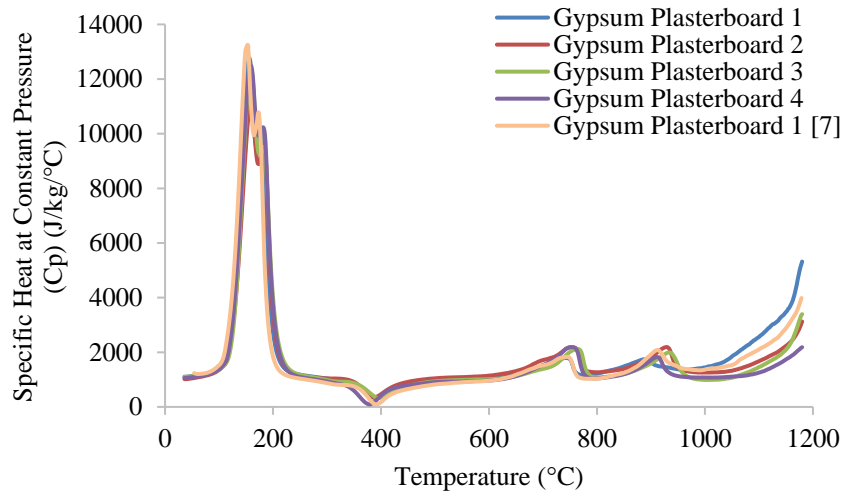


(a) Specific Heat at Constant Pressure

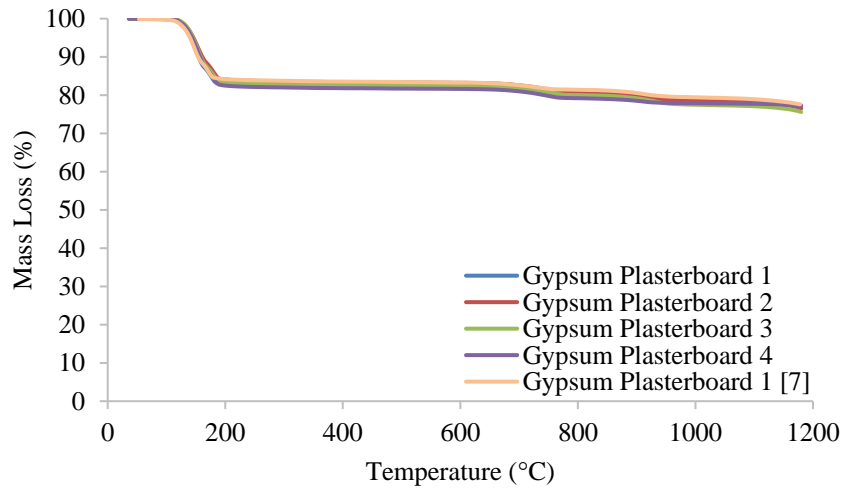


(b) Mass Loss

**Figure 7: Specific Heat and Mass Loss Plots of Gypsum Plasterboard 4**



(a) Specific Heat at Constant Pressure



(b) Mass Loss

**Figure 8: Specific Heat and Mass Loss Plots of Gypsum Plasterboards**

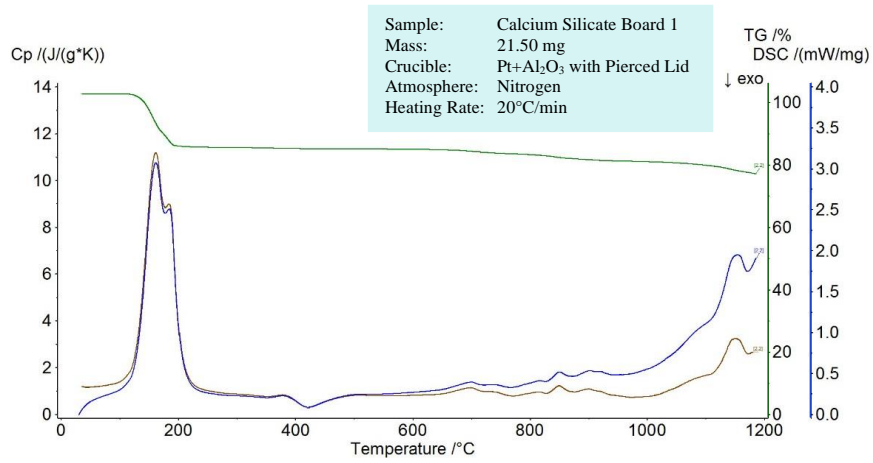
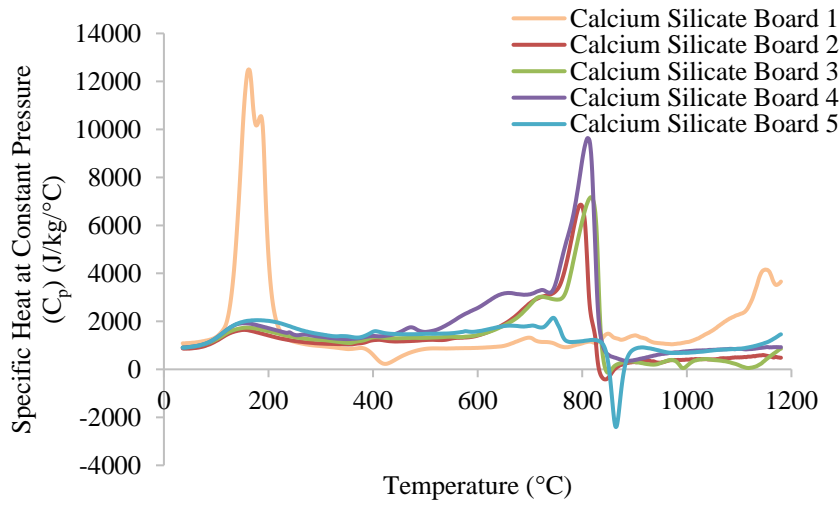
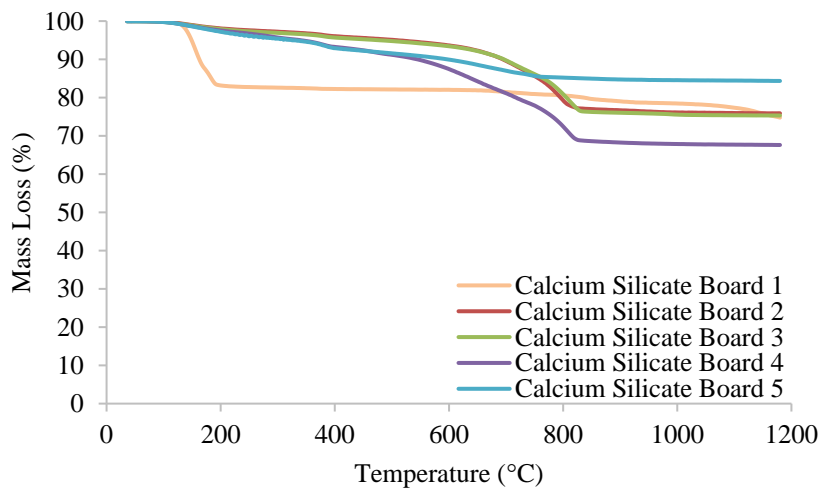


**Figure 9: STA Measurements for Calcium Silicate Board 1**

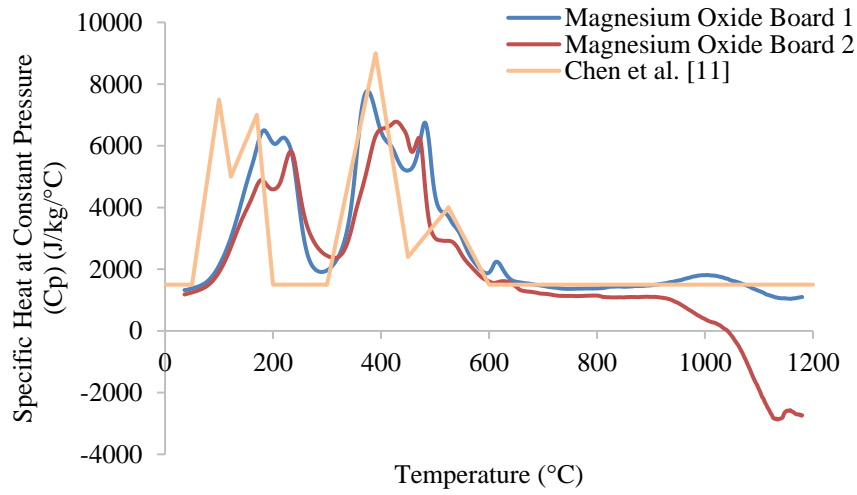


(a) Specific Heat at Constant Pressure

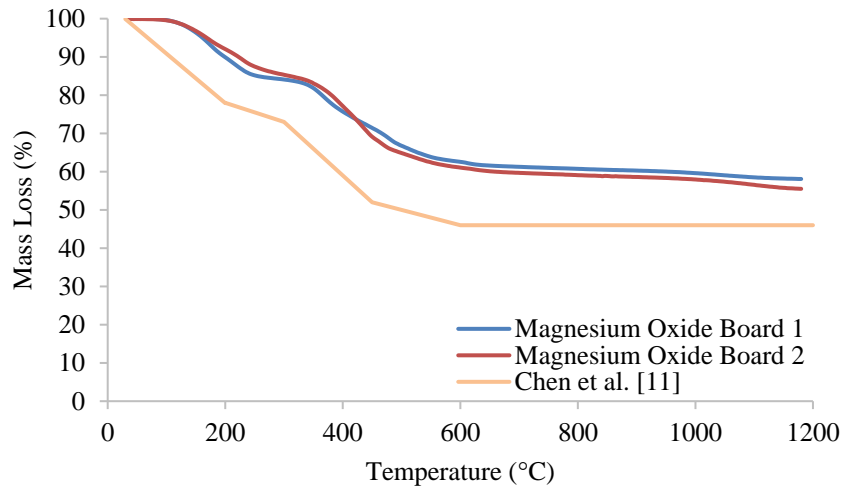


(b) Mass Loss

**Figure 10: Specific Heat and Mass Loss Plots of Calcium Silicate Boards**

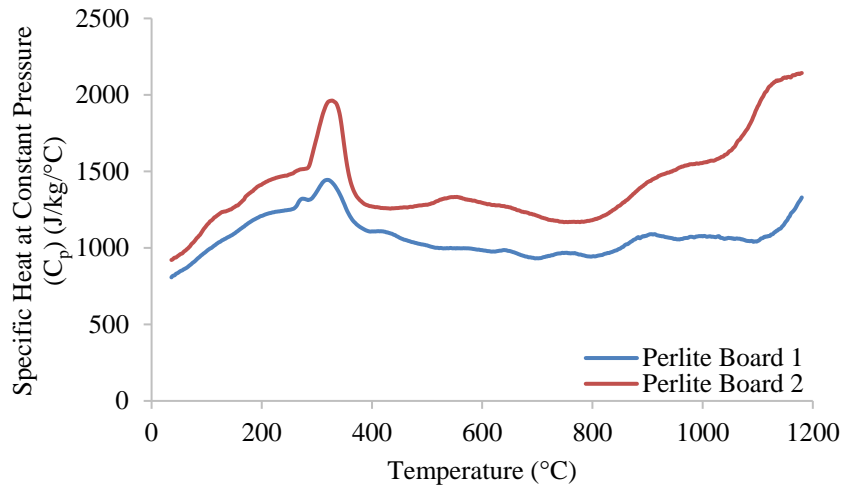


(a) Specific Heat at Constant Pressure

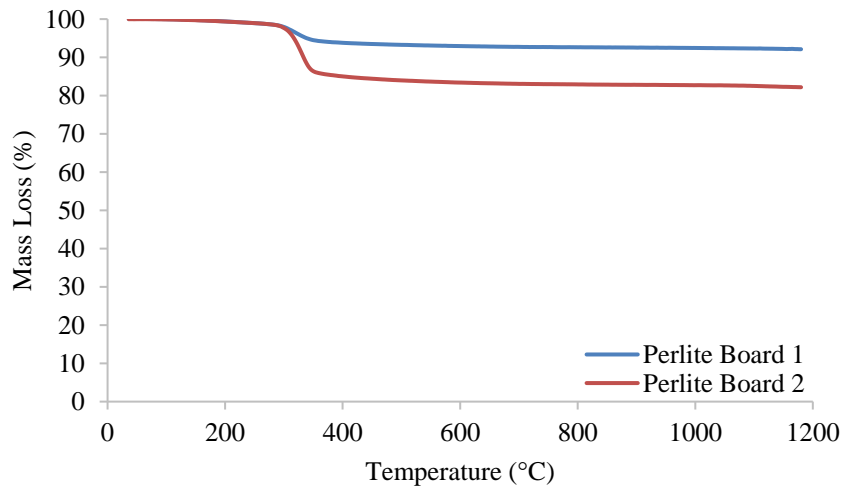


(b) Mass Loss

**Figure 11: Specific Heat and Mass Loss Plots of Magnesium Oxide Boards**

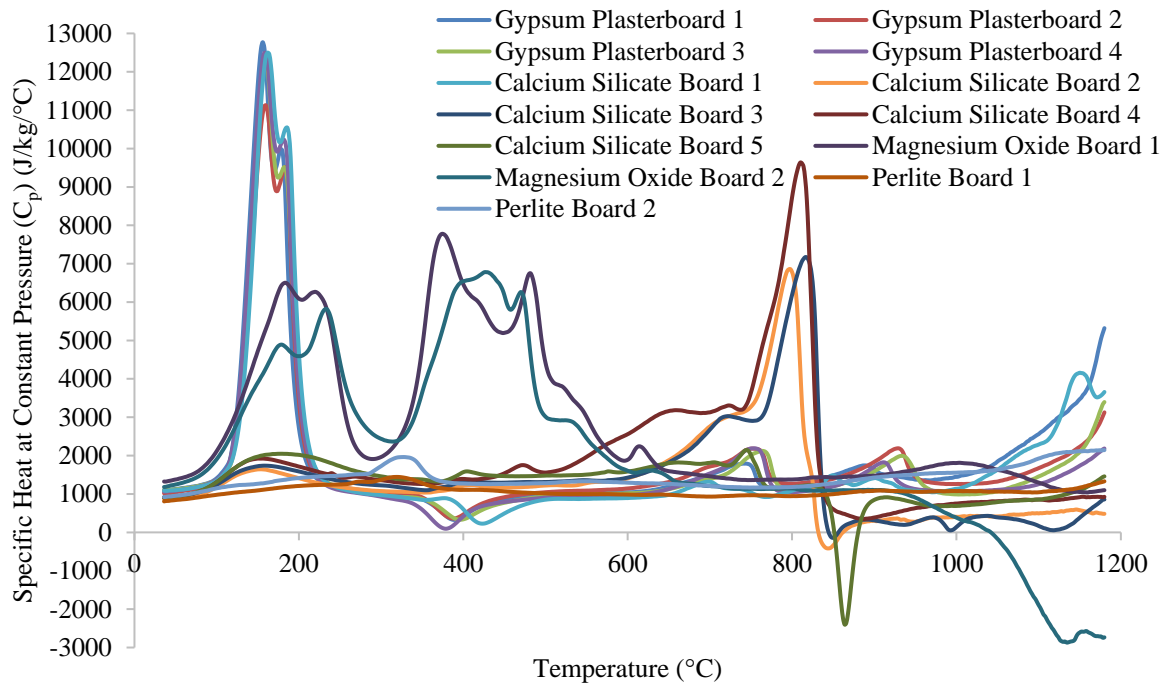


(a) Specific Heat at Constant Pressure

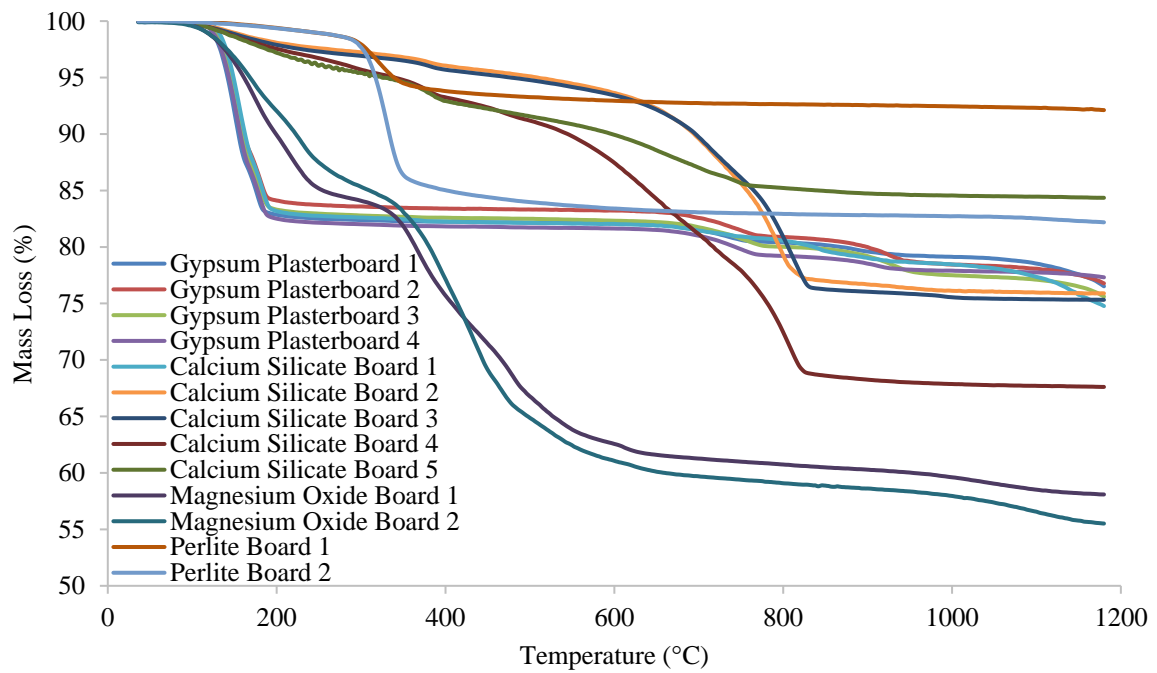


(b) Mass Loss

**Figure 12: Specific Heat and Mass Loss Plots of Perlite Boards**

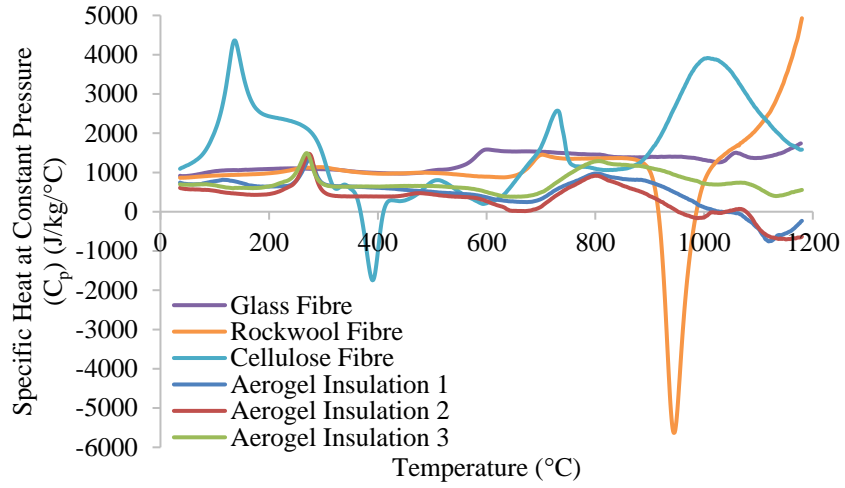


(a) Specific Heat at Constant Pressure

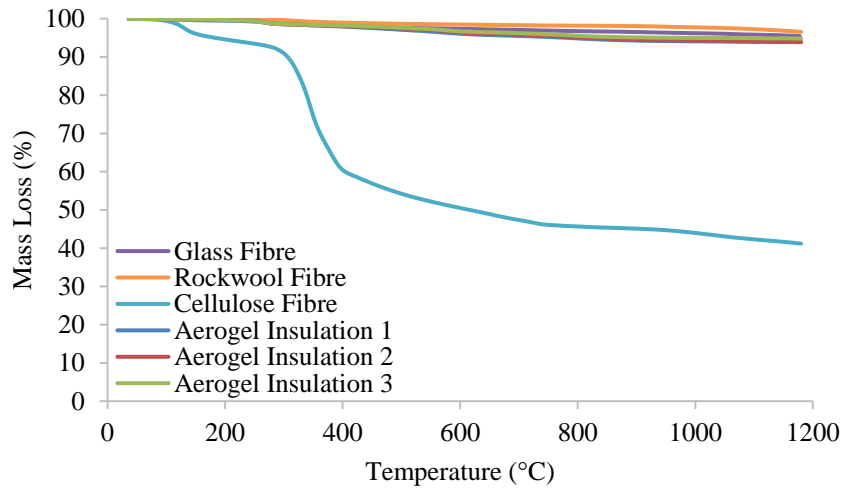


(b) Mass Loss

**Figure 13: Specific Heat and Mass Loss Plots of Fire Resistant Boards**



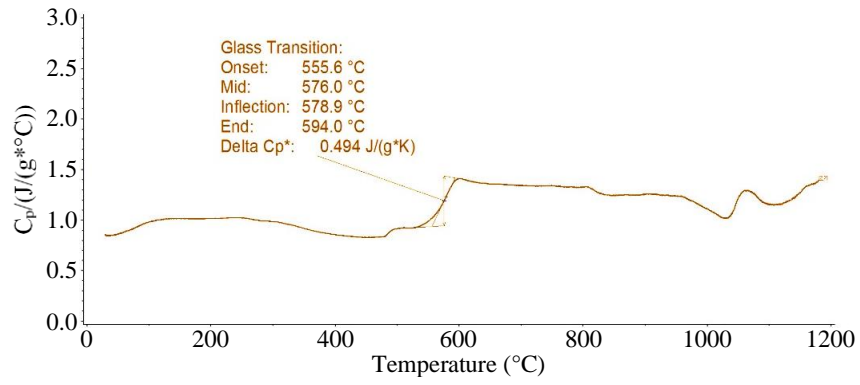
(a) Specific Heat at Constant Pressure



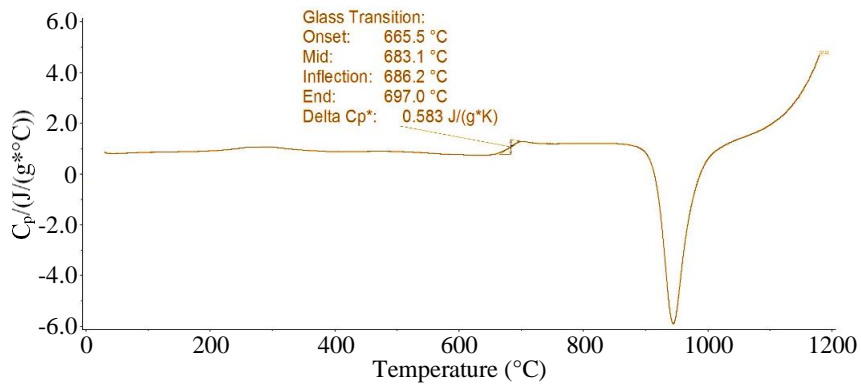
(b) Mass Loss

**Figure 14: Specific Heat and Mass Loss Plots of Insulation Materials**



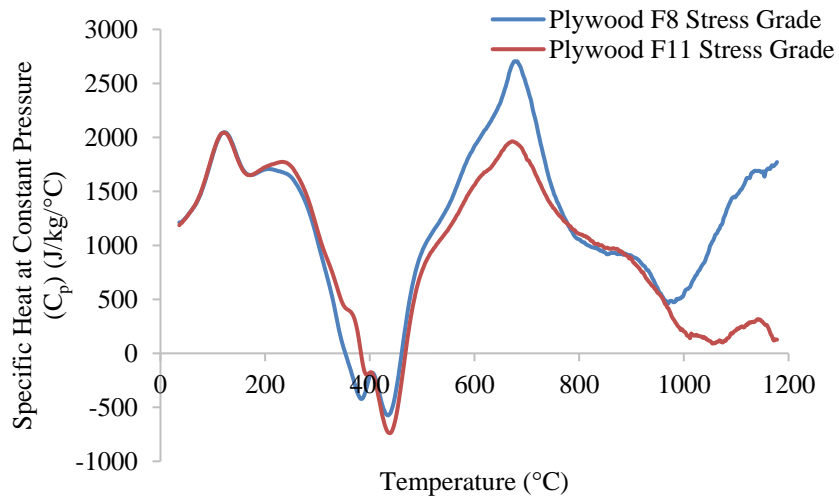


(a) Glass Fibre Insulation

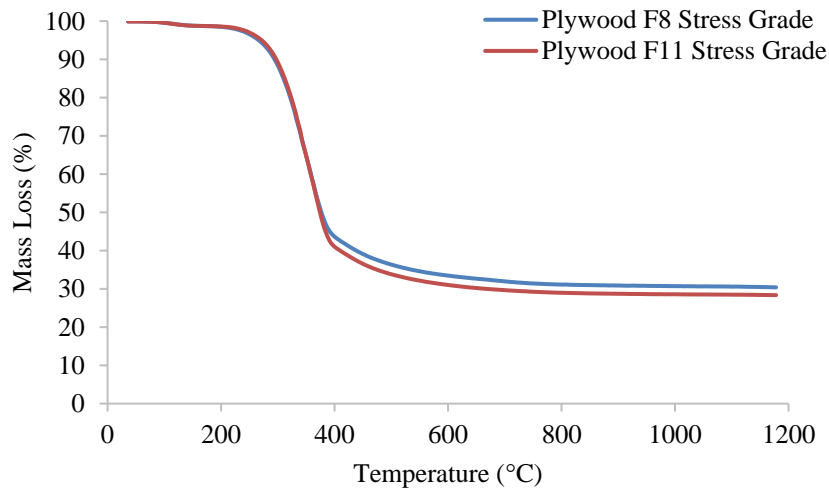


(b) Rockwool Fibre Insulation

**Figure 15: Transition Temperatures of Insulation Samples**



(a) Specific Heat at Constant Pressure



(b) Mass Loss

**Figure 16: Specific Heat and Mass Loss Plots of Plywood**

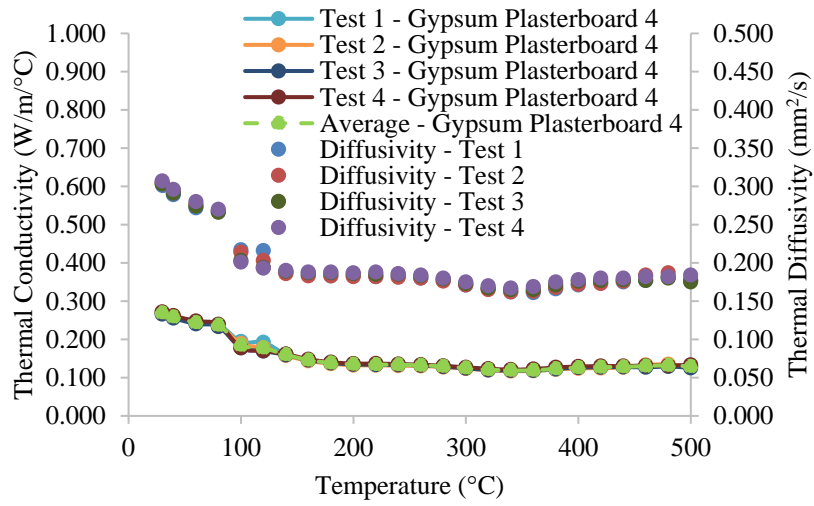
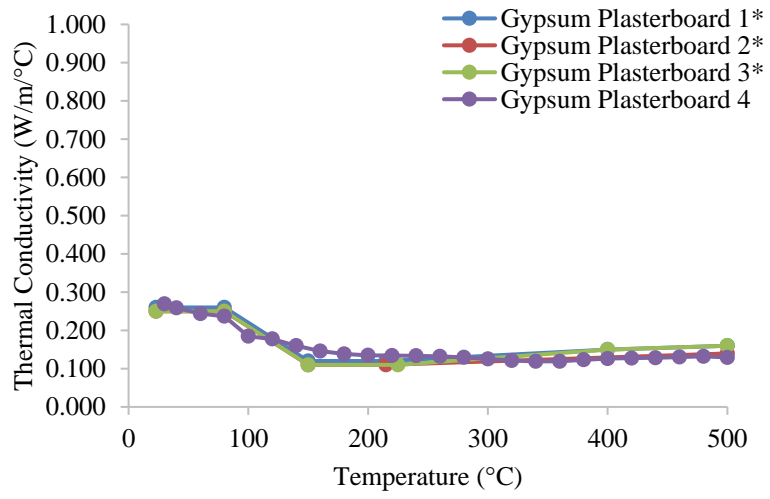
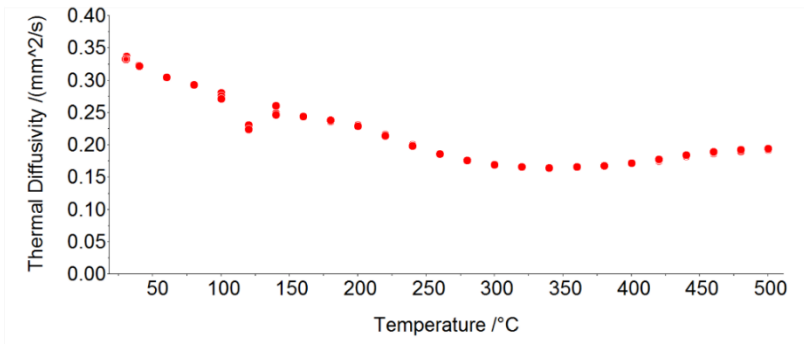


**Figure 17: Thermal Diffusivity and Thermal Conductivity Plots of Gypsum Plasterboard 4**

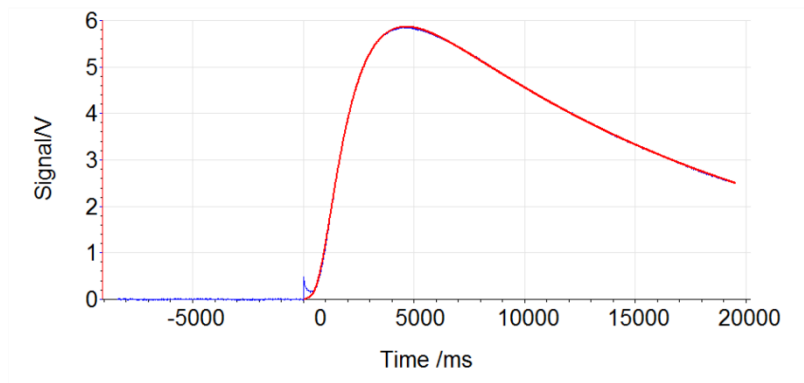


Note: \* Values of Gypsum Plasterboards 1 to 3 are from [7].

**Figure 18: Thermal Conductivity Plots of Gypsum Plasterboards**

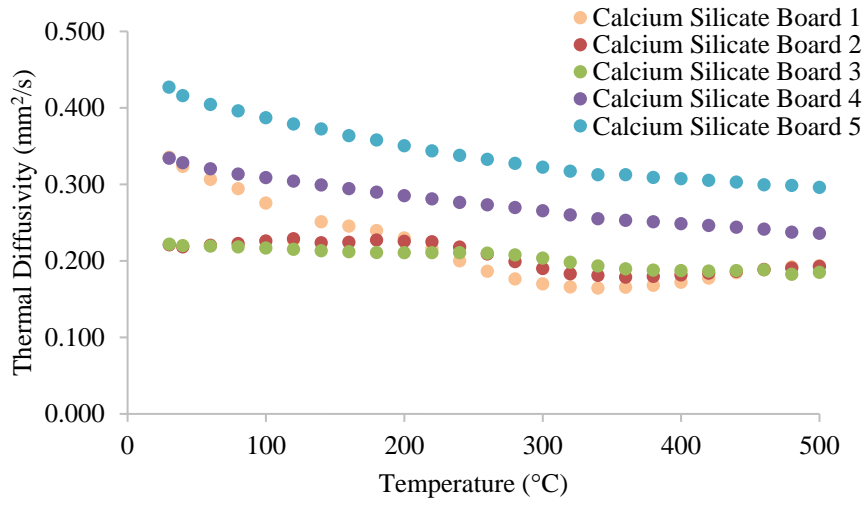


(a) Thermal Diffusivity Measurements

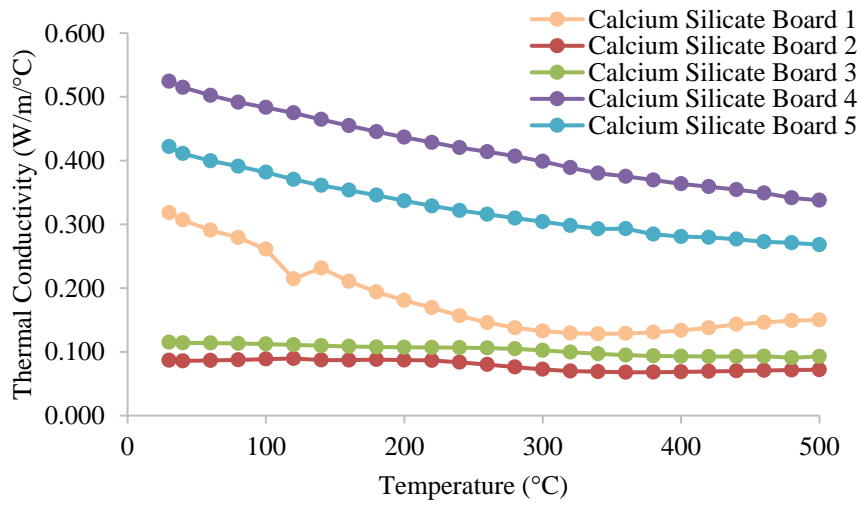


(b) Measured Temperature versus Time Curve at 160°C

**Figure 19: LFA Measurements for Calcium Silicate Board 1**



(a) Thermal Diffusivity for Calcium Silicate Boards



(b) Thermal Conductivity for Calcium Silicate Boards

**Figure 20: Thermal Diffusivity and Thermal Conductivity Plots of Calcium Silicate Boards**

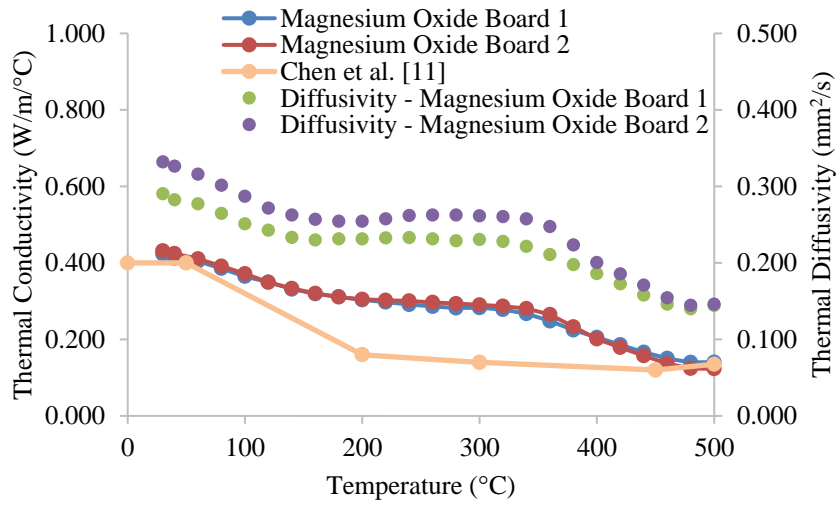


**Figure 21: Thermal Diffusivity and Thermal Conductivity Plots of Magnesium Oxide Boards**

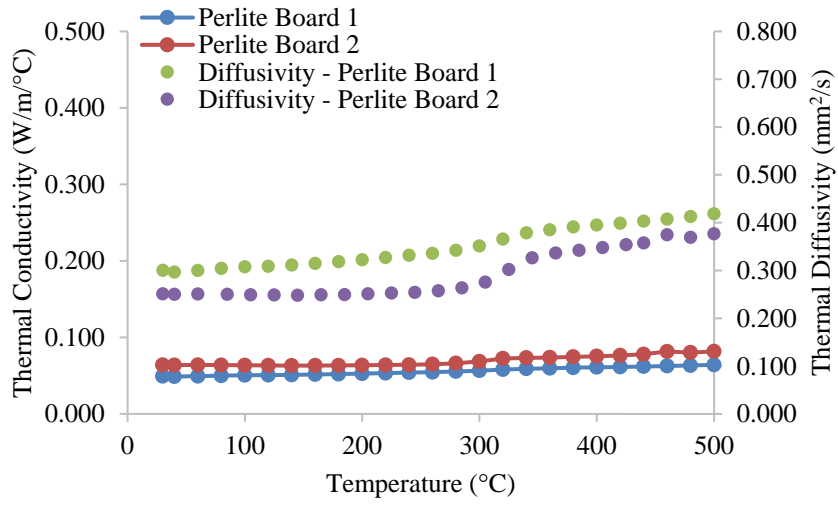


**Figure 22: Thermal Diffusivity and Thermal Conductivity Plots of Perlite Boards**



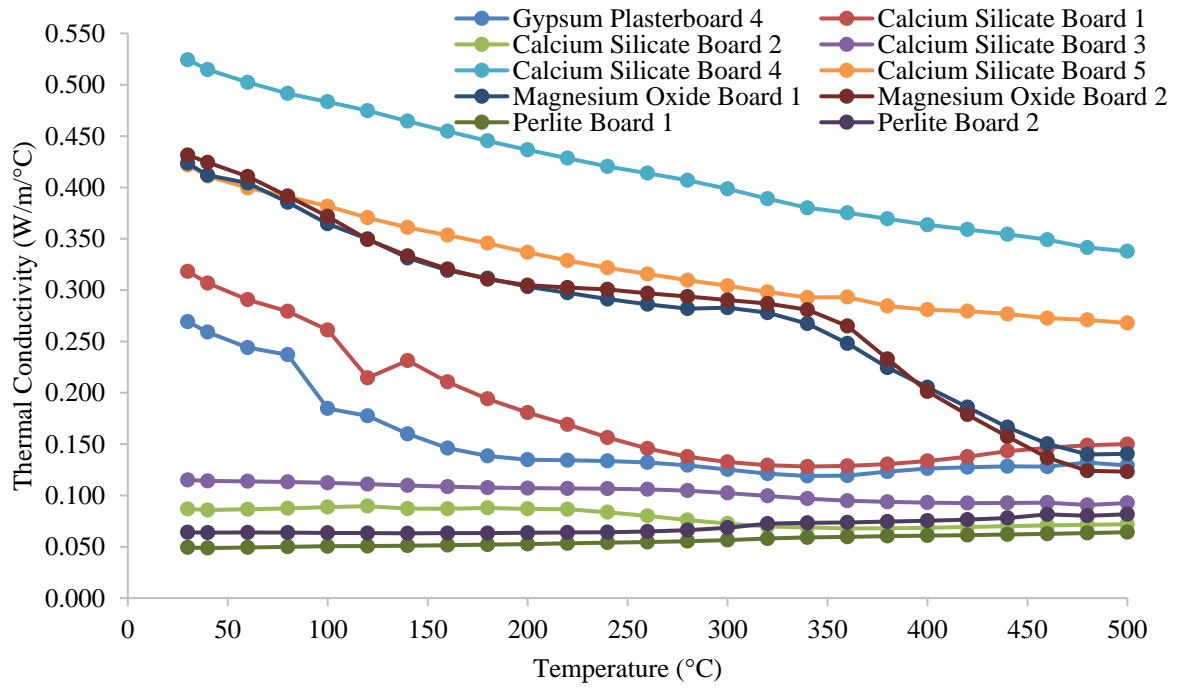


**Figure 23: Thermal Conductivity Plots of Fire Resistant Boards**

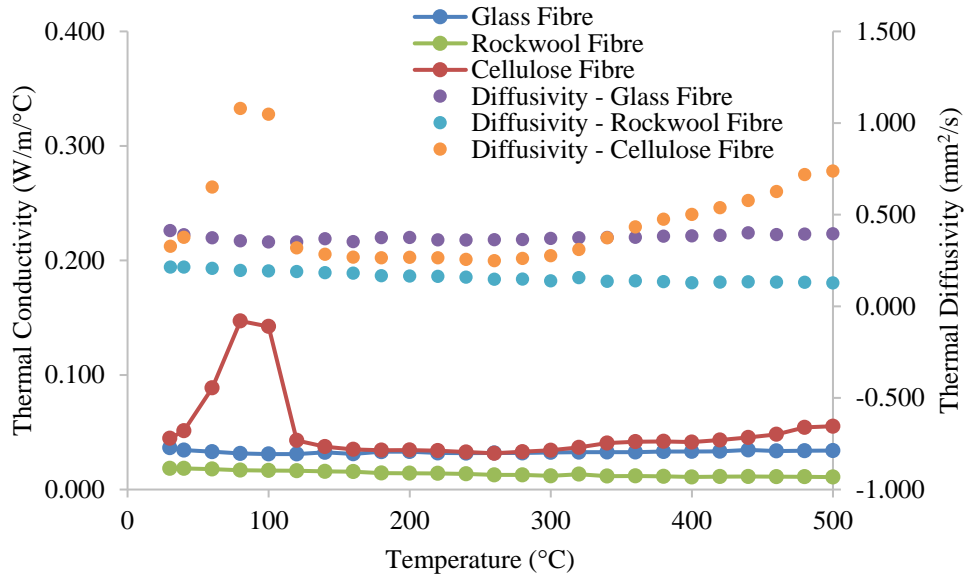


**Figure 24: Thermal Diffusivity and Thermal Conductivity Plots of Insulation Materials**

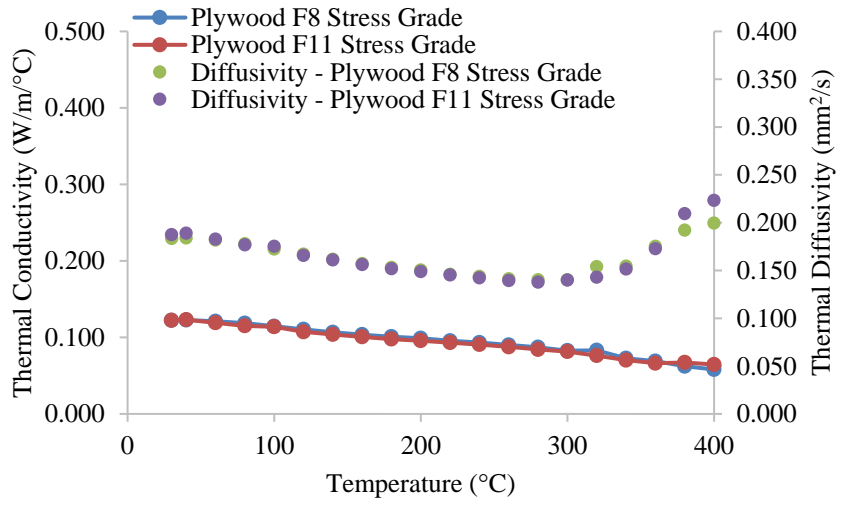
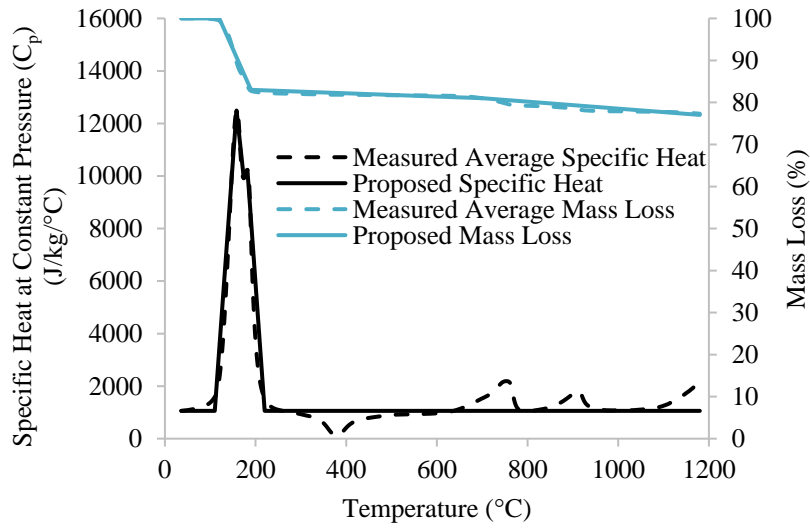
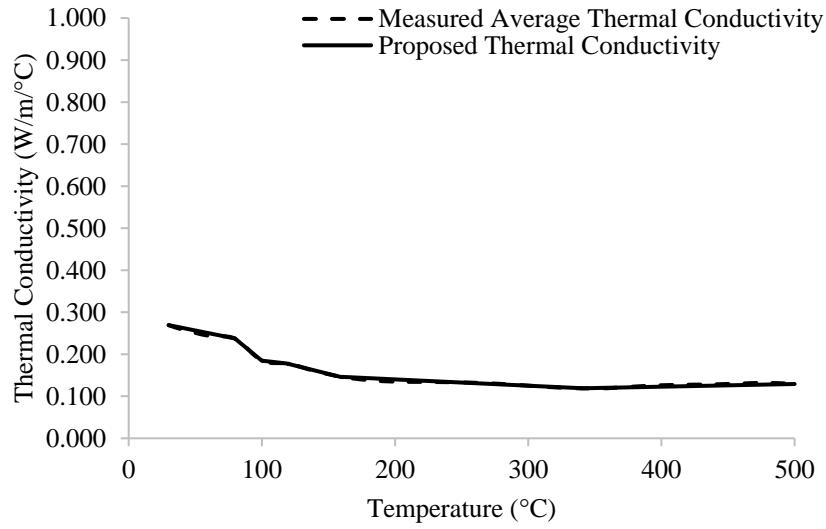


**Figure 25: Thermal Diffusivity and Thermal Conductivity Plots of Plywoods**

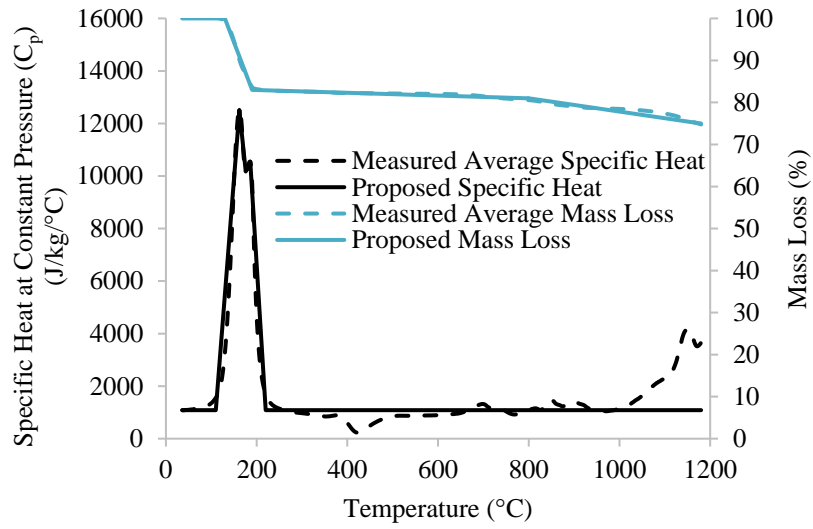


(a) Specific Heat and Mass Loss

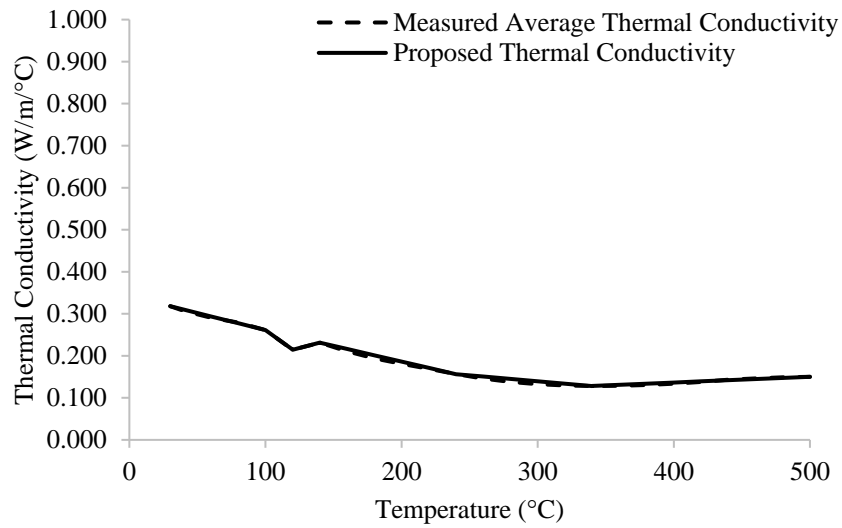


(b) Thermal Conductivity

**Figure 26: Proposed Models for Gypsum Plasterboard 4**

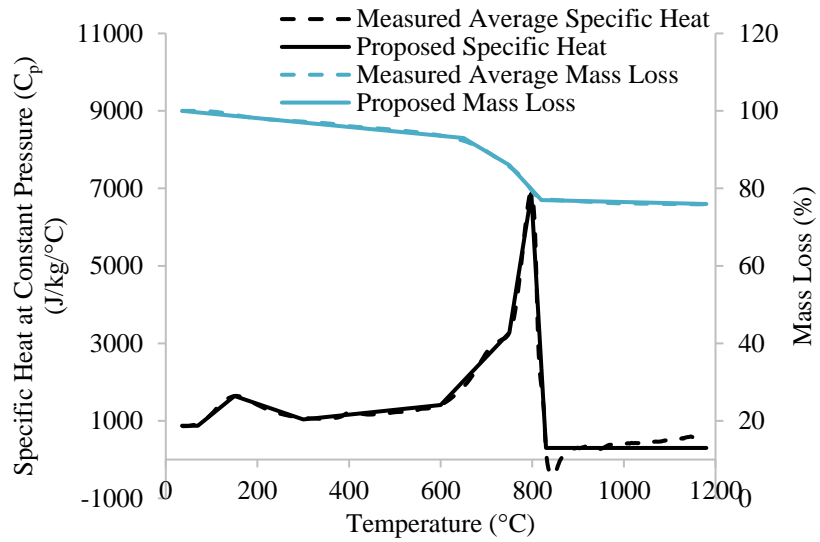


(a) Specific Heat and Mass Loss

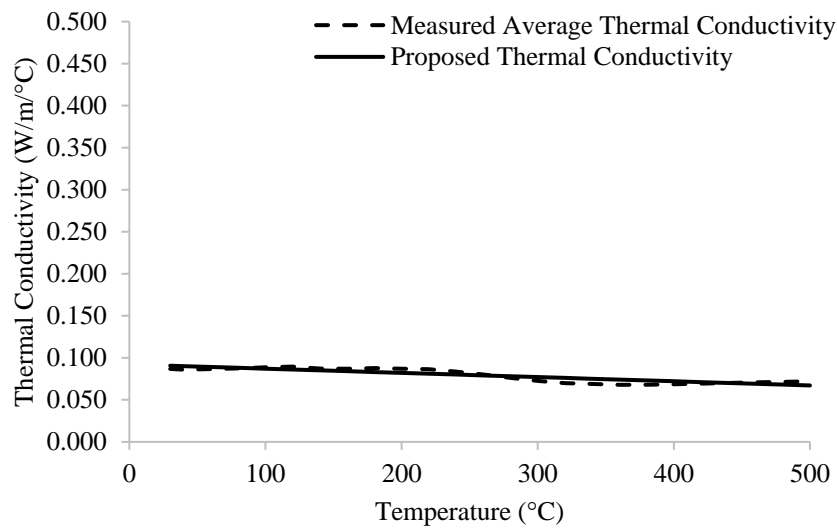


(b) Thermal Conductivity

**Figure 27: Proposed Models for Calcium Silicate Board 1**

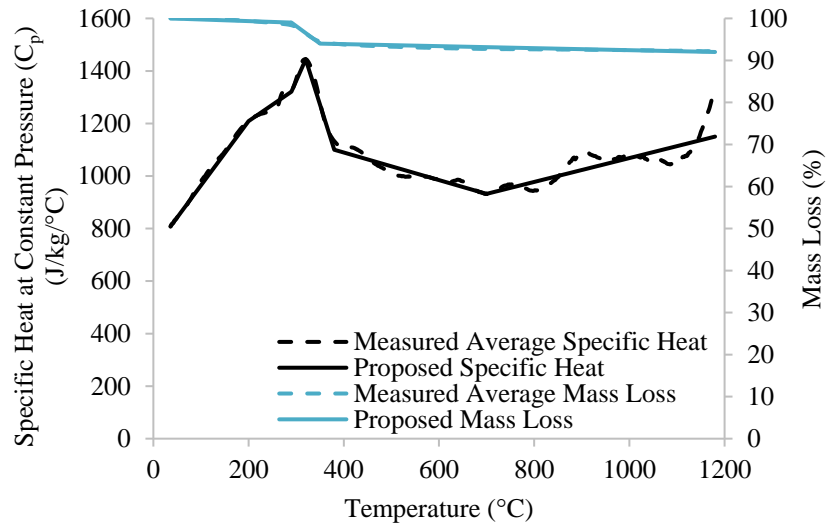


(a) Specific Heat and Mass Loss

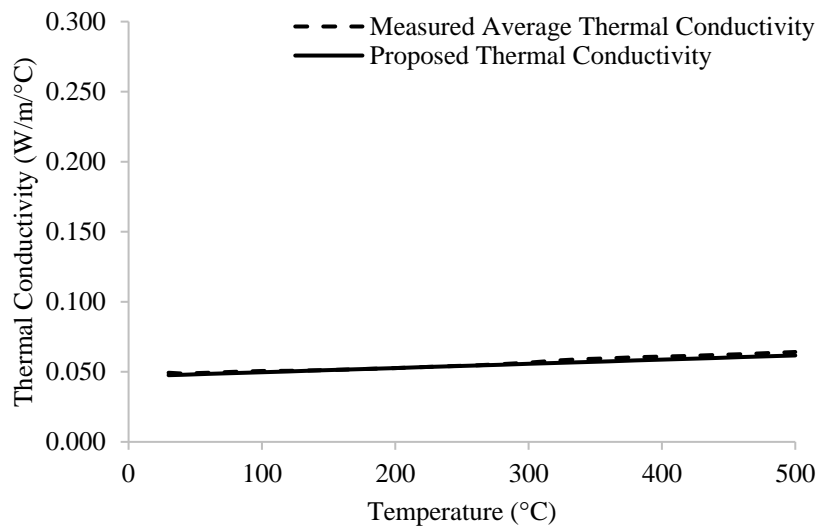


(b) Thermal Conductivity

**Figure 28: Proposed Models for Calcium Silicate Board 2**

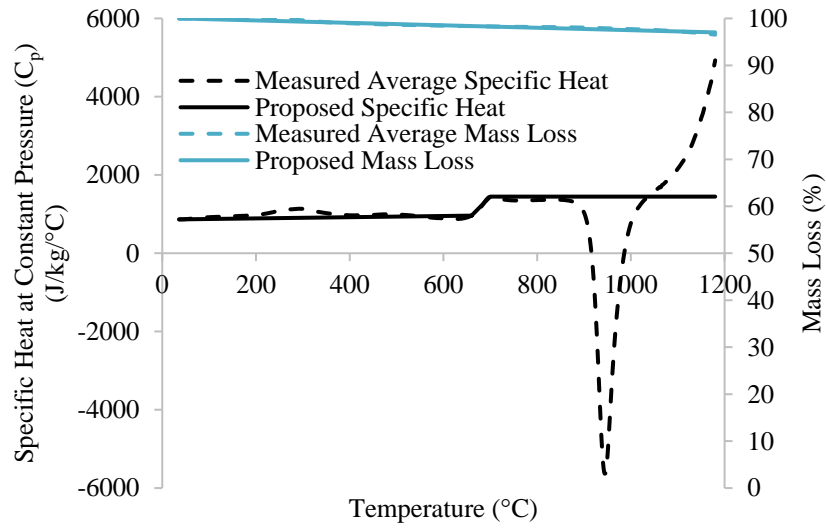


(a) Specific Heat and Mass Loss

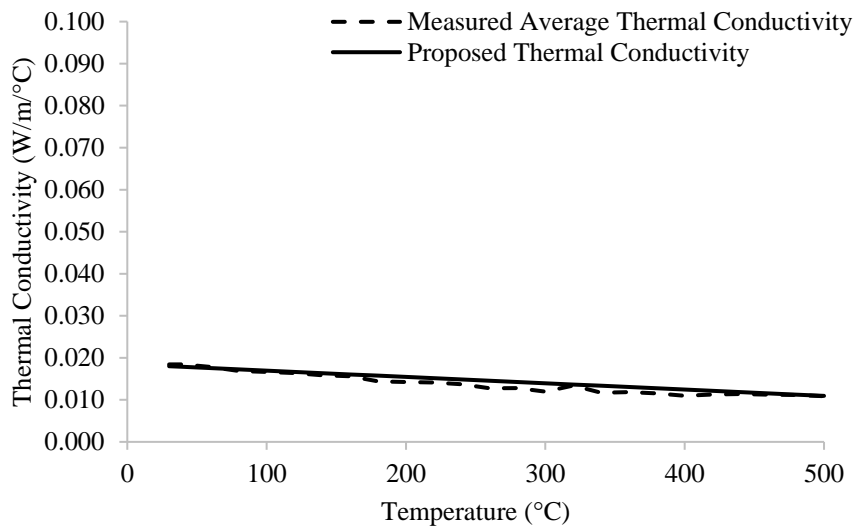


(b) Thermal Conductivity

**Figure 29: Proposed Models for Perlite Board 1**



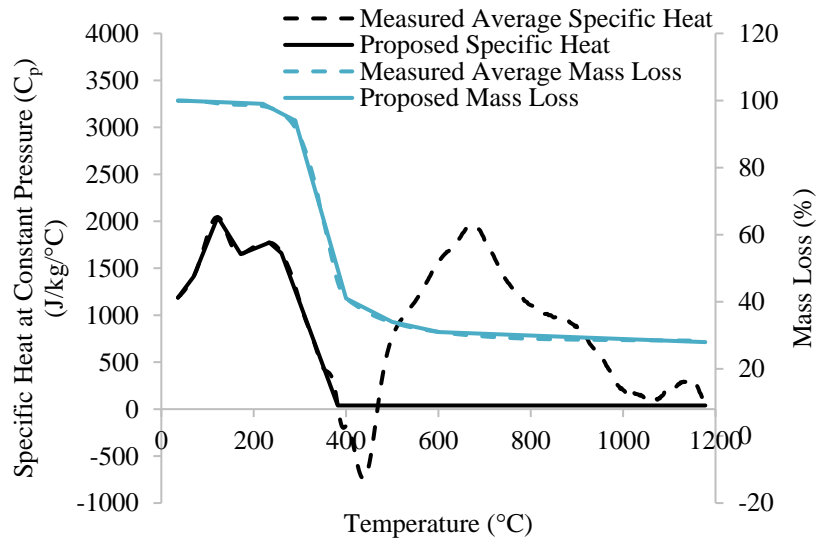
(a) Specific Heat and Mass Loss



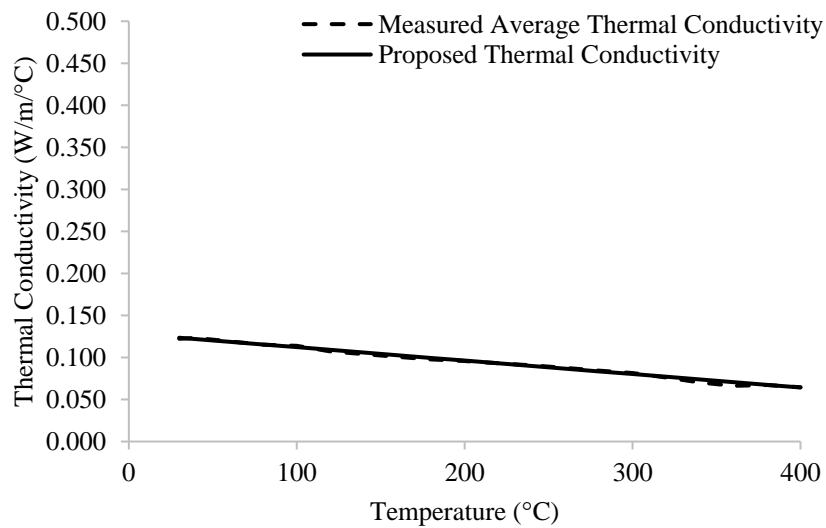
(b) Thermal Conductivity

**Figure 30: Proposed Models for Rockwool Fibre Insulation**





(a) Specific Heat and Mass Loss



(b) Thermal Conductivity

**Figure 31: Proposed Models for Plywood F11 Stress Grade**